

Desulfurization of Natural Gas for Fuel Cells

Problem Presenter

Emma Campbell, Bloom Energy

Report Editor

David A. Edwards, University of Delaware

Thirty-First Annual Workshop on Mathematical Problems in Industry
June 22–26, 2015
University of Delaware

Table of Contents

Preface	ii
Model Formulation; Asymptotics <i>D. A. Edwards</i>	1
Integrodifferential Formulation <i>B. Emerick, D. Rumschitzki</i>	28
Homogenization of Flow Equations over Pore Scale <i>C. Breward, R. O. Moore, C. Raymond</i>	34
Numerical Simulations <i>D. W. Schwendeman</i>	39

Preface

At the 31st Annual Workshop on Mathematical Problems in Industry (MPI), Emma Campbell of Bloom Energy presented a problem concerning the desulfurization of natural gas used as feedstock for fuel cells.

This manuscript is really a collection of reports from teams in the group working on several aspects of the problem. Here is a brief summary of each:

1. Edwards wrote up the main results that the bulk of the group generated during the week. His chapter contains an outline of the general problem, scales the relevant variables, and presents some results in various asymptotic limits.
2. Emerick and Rumschitzki manipulate the governing equations to obtain an integrodifferential formulation of the evolution of the number of active sites.
3. Breward, Moore, and Raymond generate additional evolution equations for the relevant quantities, and solve them in some asymptotic limits.
4. Schwendeman presents and interprets some numerical simulations of the equations, and provides some guidance as to how to make the laboratory and field results match.

In addition to the authors of these reports, the following people participated in the group discussions:

- Ivan Christov, Los Alamos National Laboratory
- Michael DePersio, University of Delaware
- Hannah Dewey, Rensselaer Polytechnic Institute
- Pavel Dubovski, Stevens Institute of Technology
- Rachel Grotheer, Clemson University
- Joseph Hibdon, Northeastern Illinois University
- Matthew Moye, New Jersey Institute of Technology
- Jacob Ortega-Gingrich, University of Washington
- Aminur Rahman, New Jersey Institute of Technology

Model Formulation; Asymptotics

David A. Edwards, University of Delaware

NOTE: Though Edwards wrote up this section, it is a summary of the week's work of the entire group (enumerated in the preface).

Section 1: Introduction

Fuel cells use hydrogen gas to produce electricity. Bloom Energy makes fuel cells that obtain their hydrogen gas from the hydrocarbons in natural gas. Sulfur is added to natural gas in order to produce odors that make leaks detectable. Typical amounts of sulfur in natural gas are between 1–5 parts per million by volume. Unfortunately, sulfur degrades the fuel cell components, and so must be filtered out of the natural gas feedstock. The gas that reaches the next component in the fuel cell must have sulfur levels as low as possible. Output concentrations in the low parts per *billion* (ppb) range are desirable.

The sulfur is removed from the gas through chemisorption (binding in a chemical reaction) or physisorption (absorption/adhesion to a surface). The desulfurization process typically occurs in beds filled with porous particles (beads) that absorb the sulfur. For our purposes, the bed may be considered as a rectangular channel of length L (see Fig. 1.1).

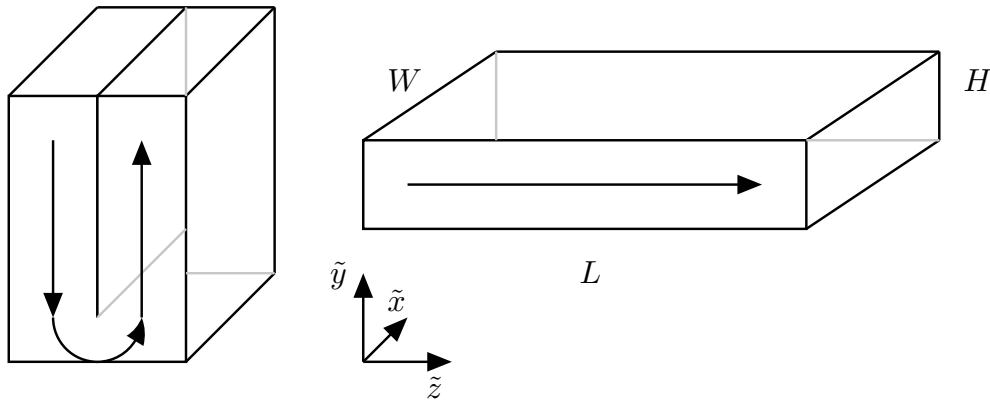


FIGURE 1.1. Left: Actual bed geometry. Right: Idealized bed geometry. Arrow indicates direction of flow.

In the field, these beds are connected in series. Each bed absorbs a certain fraction of the sulfur, and then the partially-purified gas flows to the next bed. A bed is said to have failed if

$$\frac{\tilde{C}(L)}{\tilde{C}(0)} = \frac{\tilde{C}(L)}{C_0} > C_B, \quad (1.1)$$

where \tilde{C} is the concentration of sulfur (for now assumed to be independent of \tilde{x} and \tilde{y}), and the subscript “B” stands for “breakout”. Note that C_0 is the feed concentration of sulfur. In the field, it is observed that only a few percent (by weight) of the absorbent beads is sulfur at the breakout time.

The particles in the beds can be spherical, oblate spheroid, or tubular in nature. Typical dimensions are from 1.5–4 mm. Different varieties of particles can be used; these are typically arranged in series within the beds.

In the field, the breakout time \tilde{t}_B is typically on the order of months or years, so in order to test different varieties and mixtures of particles it is best to construct laboratory

tests with smaller values of \tilde{t}_B . These tests are typically run with a larger sulfur feed input C_0 or a higher flow rate Q . It is also possible to grind the particles, thus increasing the effective reacting surface area in the bed. However, the results of these tests (in particular, which of two possible bed compositions lasts longer) do not always comport with the results in the field.

There are many reasons why this could be. In the laboratory, a standard of 50 ppb is used, and is detected by gas chromatography. In the field, samples are sent to several certified laboratories and the thresholds are much lower.

By modeling the desulfurization process, we hope to obtain insight that will allow Bloom to design laboratory protocols to eliminate this discrepancy.

Section 2: A Toy Problem

In order to understand the underlying dynamics, we consider a few toy problems.

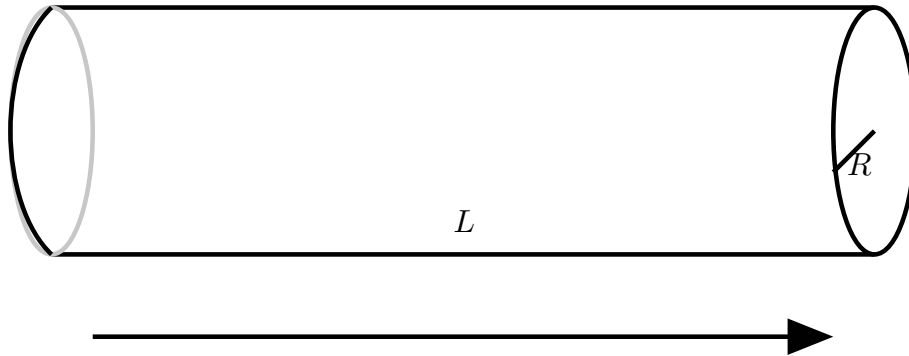


FIGURE 2.1. Cylindrical tube. Arrow indicates direction of flow.

First, consider flow down a channel of radius R and length L (see Fig. 2.1), where $R \ll L$. We may assume unidirectional plug flow with constant velocity U in the \tilde{z} -direction. This is consistent with Darcy's Law for the flow; the Reynolds number here is not small (see the Appendix).

In this case, diffusion in the \tilde{z} -direction can be neglected and the flow equation is given by

$$\frac{\partial \tilde{C}}{\partial \tilde{t}} + U \frac{\partial \tilde{C}}{\partial \tilde{z}} = \frac{D}{\tilde{r}} \frac{\partial}{\partial \tilde{r}} \left(\tilde{r} \frac{\partial \tilde{C}}{\partial \tilde{r}} \right), \quad (2.1)$$

where D is the diffusion coefficient of sulfur in natural gas. At the surface $\tilde{r} = R$, any sulfur molecule diffusing to the surface binds to an active (empty) reacting site (concentration \tilde{a}):

$$D \frac{\partial \tilde{C}}{\partial \tilde{r}}(R, \tilde{z}, \tilde{t}) = \frac{\partial \tilde{a}}{\partial \tilde{t}}. \quad (2.2)$$

We note that since \tilde{a} is a surface concentration, its units are moles/area, not moles/volume like \tilde{C} . The active reacting sites evolve according to the following irreversible kinetic law:

$$\frac{\partial \tilde{a}}{\partial \tilde{t}} = -\tilde{k}(\tilde{z}) \tilde{C}(R, \tilde{z}, \tilde{t}) \tilde{a}, \quad (2.3)$$

where $\tilde{k}(\tilde{z})$ is a rate constant. Here we allow \tilde{k} to vary with \tilde{z} to model the various species of reacting beads inside the device. However these variations are on a much larger spatial scale (usually only three different species occupy the bed) and will be discontinuous (as each species occupies its own region, and they do not mix).

Introducing scalings to simplify the problem, we let

$$C(r, z, t) = \frac{\tilde{C}(\tilde{r}, \tilde{z}, \tilde{t})}{C_0}, \quad a(z, t) = \frac{\tilde{a}(\tilde{z}, \tilde{t})}{a_{\max}}, \quad r = \frac{\tilde{r}}{R}, \quad z = \frac{\tilde{z}}{L}, \quad t = \frac{\tilde{t}}{t_*}, \quad k(z) = \frac{\tilde{k}(\tilde{z})}{k_0}, \quad (2.4a)$$

where a_{\max} is the total number of binding sites available on the surface of the cylinder and k_0 is a characteristic rate constant. (In practice, we would like it to be the largest one around, so $k(z) \leq 1$.) The characteristic time scale t_* is arbitrary for now, and

$$C_0 = \tilde{C}(\tilde{r}, 0, \tilde{t}) \quad (2.4b)$$

is the inlet concentration.

Substituting (2.4) into (2.1), we have

$$\begin{aligned} \frac{C_0}{t_*} \frac{\partial C}{\partial t} + \frac{UC_0}{L} \frac{\partial C}{\partial z} &= \frac{DC_0}{R^2} \frac{1}{r} \frac{\partial}{\partial r} \left(r \frac{\partial C}{\partial r} \right) \\ \frac{\partial C}{\partial t} + \frac{Ut_*}{L} \frac{\partial C}{\partial z} &= \frac{Dt_*}{R^2} \frac{1}{r} \frac{\partial}{\partial r} \left(r \frac{\partial C}{\partial r} \right). \end{aligned} \quad (2.5)$$

Equation (2.5) motivates two possible choices for the time scale. If we let

$$t_* = t_c = \left(\frac{U}{L} \right)^{-1}, \quad (2.6)$$

then we are choosing the *convective* time scale, which balances the two terms on the left-hand side (evolution and convection). If we let

$$t_* = t_d = \left(\frac{D}{R^2} \right)^{-1}, \quad (2.7)$$

then we are choosing the *diffusive* time scale, which balances evolution and diffusion. In either case, the coefficient of the non-balanced term will depend on the *Péclet number*

$$\text{Pe} = \frac{U/L}{D/R^2} = \frac{\text{convection rate}}{\text{diffusion rate}} = \frac{t_d}{t_c}. \quad (2.8)$$

Substituting (2.4) into (2.2), we have

$$\begin{aligned} \frac{DC_0}{R} \frac{\partial C}{\partial r}(1, z, t) &= \frac{a_{\max}}{t_*} \frac{\partial a}{\partial t} \\ \frac{t_*}{t_d} \frac{C_0}{a_{\max}/R} \frac{\partial C}{\partial r}(1, z, t) &= \frac{\partial a}{\partial t}. \end{aligned} \quad (2.9)$$

Equation (2.9) motivates another possible choice for the time scale, namely

$$t_* = \frac{a_{\max}/R}{C_0} t_d. \quad (2.10)$$

Note that the numerator of the coefficient essentially converts the area concentration to a volume concentration (since the receptors are distributed along a circumference of $2\pi R$).

Lastly, substituting (2.4) into (2.3), we obtain

$$\begin{aligned}\frac{a_{\max}}{t_*} \frac{\partial a}{\partial t} &= -a_{\max} C_0 k_0 k(z) C(1, z, t) a \\ \frac{\partial a}{\partial t} &= -k_0 C_0 t_* k(z) C(1, z, t) a.\end{aligned}\tag{2.11}$$

Equation (2.11) motivates another possible choice for the time scale, namely

$$t_* = t_k = (C_0 k_0)^{-1},\tag{2.12}$$

which is the *reacting time scale*.

These multiple time scales indicate one explanation for the laboratory discrepancy. Consider two possible bed compositions. In one (X), the slowest rate is the reaction rate; in the other (Y), the slowest rate is the diffusion rate. Suppose that in the field, X is superior (larger breakout time). Now consider a lab experiment where we retain the same compositions, but increase the feed concentration C_0 in an attempt to reduce the breakout time for testing purposes. Increasing C_0 will increase the reaction rate, thereby reducing the breakout time for X, which is limited by the reaction rate, but not for Y, which is limited by the diffusion rate. So in the lab, Y may look superior because its breakout time is now longer.

To compensate for this, in an ideal laboratory setting we would design our experiment so that each of the rates is increased by the same factor. That would imply keeping Pe constant. Hence changing L (as we do in the lab experiment), will necessitate a change in U . Changing C_0 should be avoided, since we must also keep the following ratio constant:

$$\frac{t_d}{t_k} = \frac{k_0 C_0}{D/R^2} = \frac{\text{reaction rate}}{\text{diffusion rate}} = Da,\tag{2.13}$$

where Da denotes the Damköhler number. This means that changing C_0 would force a change in R , which we might be able to do by grinding up the particles. This is to be avoided if possible, because some of the particles are coated, and grinding them up would change the position of the coating and hence the absorption properties of the particles. Moreover, we also have to keep the ratio in (2.10) constant, which would necessitate changing a_{\max} . (This may also happen as a result of changing R .)

This trouble could be obviated somewhat if we had an inkling of which rates would be slowest. Then we could focus on balancing that ratio, instead of worrying about all three ratios at once.

We conclude this section by noting that the problem as posed is unrealistic. With plug flow, the evolution equation is independent of r , which means that the left-hand side of (2.2) would be zero, which means that there would be no binding to the surface. This type of model is better when there is standard Poiseuille flow, where the velocity depends upon r , which forces a concentration gradient in r .

Section 3: Governing Equations

We examine what happens in an individual pore, and then use the result to inform a homogenized model at the vessel level. Consider an individual pore, again with the geometry in Fig. 2.1. Here we denote pore-related variables with the subscript ‘‘p’’.

The breakout phenomenon occurs when a goes to 0 in large portions of the vessel. To track the evolution of a , we choose t_k for a time scale as in (2.12). For transport in the pore, we follow the discussion in [2, §12.3.1]. In general, the pore radius is so small (on the order of nanometers, or the typical size of the mean free path), that the dominant effect is Knudsen diffusion [2, §12.2] in the \tilde{z} -direction. Knudsen diffusion describes the situation where the collisions most likely to occur are between the molecule and the pore, rather than neighboring molecules. In particular, we have that C_p is uniform across the pore, and hence depends only on z_p , the distance down the pore. Thus (2.11) becomes

$$\frac{\partial a}{\partial t} = -k(z)C_p a. \quad (3.1)$$

(a exists only in the pores, so we don’t use a subscript ‘‘p’’ for it.)

At the open end ($z_p = 0$) of any pore at position z , the concentration must be continuous:

$$C_p(0, t; z) = C(z, t). \quad (3.2)$$

Therefore both C_p and a will depend parametrically on z , not only through k but also through coupling to the bulk.

This diffusion in the pore is balanced by reaction to a on its surface. Hence we have

$$D \frac{\partial^2 (\pi R_p^2 \tilde{C}_p)}{\partial \tilde{z}^2} = - \frac{\partial (2\pi R_p \tilde{a})}{\partial \tilde{t}}. \quad (3.3)$$

Here the parenthetical quantity on the left-hand side represents the total sulfur in the cross-sectional slice, while the parenthetical quantity on the right-hand side represents the total binding in the circumference around that slice. Substituting in our chosen scalings, we obtain

$$\begin{aligned} D\pi R_p^2 \frac{C_0}{L_p^2} \frac{\partial^2 C_p}{\partial z_p^2} &= -2\pi R_p a_{\max} k_0 C_0 \frac{\partial a}{\partial t} \\ \frac{\partial^2 C_p}{\partial z_p^2} &= - \frac{2a_{\max} k_0 L_p^2}{DR_p} (-k(z)C_p a) \\ &= h_T^2 k(z)C_p a, \quad h_T = L_p \sqrt{\frac{2k_0 a_{\max}}{DR_p}} = \frac{\text{reaction rate}}{\text{diffusion rate}}, \end{aligned} \quad (3.4)$$

where we have used (3.1). h_T is called the *Thiele modulus* [2, p. 440].

To calculate the typical length of a pore, we use the following rule of thumb: we divide the volume of the bead by its surface area. Since we are considering cylindrical beads, we have the following:

$$L_p = \frac{\pi R_b^2 L_b}{2\pi R_b L_b} = \frac{R_b}{2}, \quad (3.5)$$

where the subscript “b” refers to bead. The surface area of the ends of the pellet is considered to be negligible because $R_b \ll L_b$. (For more details on parameter values, see the Appendix.) Substituting (3.5) into (3.4), yields

$$h_T = \frac{R_b}{2} \sqrt{\frac{2k_0 a_{\max}}{DR_p}}. \quad (3.6)$$

Equation (3.4) requires two boundary conditions. We think of the pore as being a closed cylindrical tube. Hence in addition to (3.2), there can be no diffusive flux at the closed end $z = 1$, and we have

$$\frac{\partial C_p}{\partial z_p}(1, t; z) = 0. \quad (3.7)$$

Finally, we have an initial condition on a , which is given by our scaling for \tilde{a} :

$$a(z_p, 0; z) = 1. \quad (3.8)$$

In the bulk, we assume plug flow as before. Then the governing transport equation is independent of \tilde{r} and given by

$$\frac{\partial \tilde{C}}{\partial \tilde{t}} + U \frac{\partial \tilde{C}}{\partial \tilde{z}} = \frac{\text{flux}}{\text{volume in vessel}} \text{ due to pores.} \quad (3.9)$$

The right-hand side can be broken up as follows, where we use the word “hole” to denote “open end of pore”:

$$\frac{\text{flux}}{\text{volume in vessel}} = \frac{\text{flux}}{\text{area of hole}} \cdot \frac{\text{area}}{\text{pore}} \cdot \frac{\text{pores}}{\text{bead}} \cdot \frac{\text{bead}}{\text{volume in vessel}}. \quad (3.10)$$

To relate this to our previous work, we see that the flux through the open end of a single pore is given by the following:

$$\frac{\text{flux}}{\text{area of hole}} = \frac{DC_0}{L_p} \frac{\partial C_p}{\partial z_p}(0, t; z). \quad (3.11)$$

The area of the hole is trivially πR_b^2 . The number of pores per bead is given by

$$\frac{\text{pores}}{\text{bead}} = \frac{\text{total pore volume in bead}}{\text{volume of pore}} = \frac{V_b \phi_p}{V_p}, \quad (3.12)$$

where V denotes volume and ϕ_p is the void fraction of pores in the bead. The number of beads in a given volume in the vessel is given by the following:

$$\frac{\text{bead}}{\text{volume in vessel}} = \frac{1 - \phi_b}{V_b}, \quad (3.13)$$

where ϕ_b is the void fraction of beads in the vessel.

Substituting these results into (3.10) and then (3.9), we have

$$\begin{aligned} \frac{\text{flux}}{\text{volume in vessel}} &= \left[\frac{DC_0}{L_p} \frac{\partial C_p}{\partial z_p}(0) \right] \pi R_p^2 \left[\frac{\phi_p(1 - \phi_b)}{\pi R_p^2 L_p} \right] \\ \frac{\partial \tilde{C}}{\partial \tilde{t}} + U \frac{\partial \tilde{C}}{\partial \tilde{z}} &= \frac{DC_0}{R_b/2} \left[\frac{\phi_p(1 - \phi_b)}{R_b/2} \right] \frac{\partial C_p}{\partial z_p}(0, t; z). \end{aligned} \quad (3.14)$$

Substituting our previous scalings into (3.14), we obtain

$$\begin{aligned} k_0 C_0^2 \frac{\partial C}{\partial t} + \frac{UC_0}{L} \frac{\partial C}{\partial z} &= \frac{4DC_0}{R_b^2} \phi_p(1 - \phi_b) \frac{\partial C_p}{\partial z_p}(0, t; z) \\ \frac{k_0 C_0 R_b^2}{4D\phi_p(1 - \phi_b)} \frac{\partial C}{\partial t} + \frac{UR_b^2}{4D\phi_p(1 - \phi_b)L} \frac{\partial C}{\partial z} &= \frac{\partial C_p}{\partial z_p}(0, t; z) \\ \alpha_2 \left(\alpha_1 \frac{\partial C}{\partial t} + \frac{\partial C}{\partial z} \right) &= \frac{\partial C_p}{\partial z_p}(0, t; z), \end{aligned} \quad (3.15)$$

$$\alpha_1 = \frac{k_0 C_0 L}{U} = \frac{\text{convection time across vessel}}{\text{breakout? time}}, \quad (3.16a)$$

$$\alpha_2 = \frac{UR_b^2}{4D\phi_p(1 - \phi_b)L} = \frac{\text{convection rate across vessel}}{\text{diffusion rate along pore}}. \quad (3.16b)$$

Here we have made the coefficient of the right-hand side equal to 1 in order to guarantee that the sink term is included in the analysis. From the Appendix, we have that α_2 is very close to 1.

During the time of the workshop, we interpreted $k_0 C_0$ as the breakout time. Since that is on the order of months, while the convection time across the vessel is on the order of seconds, we would have $\alpha_1 \ll 1$ and the first term may be neglected. However, later asymptotic work (see §4) suggested that another, longer time scale is associated with breakout. Thus this estimate may not be correct. To tell, we need a good estimate for k_0 .

However, proceeding on that assumption, to leading order our final equation is

$$\alpha_2 \frac{\partial C}{\partial z} = \frac{\partial C_p}{\partial z_p}(0, t; z). \quad (3.17)$$

The necessary condition on C is given by the scaled version of (2.4b):

$$C(0, t) = 1. \quad (3.18)$$

Our system is thus given by (3.1), (3.4), and (3.17) subject to (3.2), (3.7), (3.8), and (3.18). This system may be solved numerically; see the chapter by Schwendeman.

We conclude this section by noting the ramifications of our analysis for laboratory experiments. In the laboratory, we wish to accelerate the reaction process and reduce the breakout time. Our analysis shows that the relevant reaction rate is kC_0 from (2.12). Therefore, in the lab they should increase the feed concentration. However, one must be careful because this could induce secondary reactions.

In order to ensure that all other time scales in the problem are untouched, one must keep α_2 constant. (α_1 is so small that changing it will not affect the experiment.) This is accomplished by setting

$$\begin{aligned} \frac{U_1}{L_1} &= \frac{U_f}{L_f} \\ \frac{Q_1}{V_1} &= \frac{Q_f}{V_f}, \end{aligned} \tag{3.19}$$

where “l” refers to the laboratory values and “f” refers to the field values. The first line can be interpreted as keeping the gas transit time through the vessel the same in both settings. The second line can be interpreted as keeping the *space velocity* (the rate at which the entire volume of the bed is replaced) the same in both settings.

Clearly the dimensionless breakout time for any bed composition will be a function of α_2 and h_T . One anomaly we were asked to explain was the fact that when comparing some pairs of compositions (say X and Y), one would work better in the lab, while the other would work better in the field. In other words,

$$t_B(\alpha_{2,f,X}; h_{T,X}) < t_B(\alpha_{2,f,Y}; h_{T,Y}) \text{ while } t_B(\alpha_{2,l,X}; h_{T,X}) > t_B(\alpha_{2,l,Y}; h_{T,Y}).$$

Further investigation is needed to see if just violating the constraint in (3.19) is sufficient to cause this phenomenon.

Section 4: An Asymptotic Discussion

Because we have no good measurements for a_{\max} , we are unsure of the size of h_T . We expect the problem to be diffusion-limited, which corresponds to the case $h_T \rightarrow \infty$. In that case, from (3.4) we have that $C_p a = 0$. There are two ways this can happen:

Case 1: $C_p = 0$

The first case we consider is when the concentration of sulfur in the pore is equal to zero. Far down the channel, we expect that the sulfur concentration in the bulk will also be zero, since the sulfur has been removed upstream. Therefore, if $C(z, t) = 0$, then $C_p = 0$ is an exact solution to our system.

However, near the upstream end of the channel, we know that $C(z, t) \neq 0$ by (3.18). Hence there must be a boundary layer near the entry of the pore to match the outer solution $C_p = 0$ to the boundary condition $C(z, t) = 0$. By choosing

$$\zeta_p = h_T z_p, \quad \hat{C}_p(\zeta_p, t) = C_p(z_p, t), \quad \hat{a}(\zeta_p, t) = a(z_p, t), \quad (4.1)$$

we have that (3.4) becomes

$$\begin{aligned} h_T^2 \frac{\partial^2 \hat{C}_p}{\partial \zeta_p^2} &= h_T^2 k(z) \hat{C}_p \hat{a} \\ \frac{\partial^2 \hat{C}_p}{\partial \zeta_p^2} &= k(z) \hat{C}_p \hat{a}, \end{aligned} \quad (4.2)$$

which is just (3.4) with $h_T = 1$. So we have basically just compressed the transition in the $h_T = O(1)$ case into a region of width $O(h_T^{-1})$.

Since in the limit of large h_T , $C_p a = 0$, we have from (3.1) that a does not evolve on the t time scale. Therefore, there must be a slow time scale where a evolves, and the boundary layer penetrates into the pore, eventually reaching the other case that satisfies (3.4), namely $a = 0$.

The scaling in (4.1) forces the flux in \hat{C}_p to be $O(h_T)$, which forces a boundary layer in z to balance (3.17). Hence the region where $C_T \neq 0$ and $C = 0$ must occur in a narrow band. This band will move down the pore on the slow time scale. Thus, we let

$$\zeta = h_T(z - z_*(\tau)), \quad \tau = t h_T^{-b} \quad \hat{C}(\zeta, \tau) = C(z, t), \quad (4.3)$$

where b is a constant yet to be determined. Substituting (4.3) into (3.17) and (3.1) yields the following:

$$\begin{aligned} \alpha_2 h_T \frac{\partial \hat{C}}{\partial \zeta} &= h_T \frac{\partial \hat{C}_p}{\partial \zeta_p}(0, \tau; \zeta) \\ \alpha_2 \frac{\partial \hat{C}}{\partial \zeta} &= \frac{\partial \hat{C}_p}{\partial \zeta_p}(0, \tau; \zeta), \\ -h_T^{1-b} \frac{dz_*}{d\tau} \frac{\partial \hat{a}}{\partial \zeta_p} + h_T^{-b} \frac{\partial \hat{a}}{\partial \tau} &= -k(z_*(\tau) + h_T^{-1} \zeta) \hat{C}_p \hat{a}. \end{aligned} \quad (4.4a)$$

The dominant term on the left-hand side is the first; to balance it with the right-hand side, we take $b = 1$ to obtain, to leading order,

$$-\frac{dz_*}{d\tau} \frac{\partial \hat{a}}{\partial \zeta_p} = -k(z_*(\tau)) \hat{C}_p \hat{a}. \quad (4.4b)$$

Equation (4.4b) also is just (3.17) with $h_T = 1$.

Case 2: $a = 0$

We next consider the other case of interest: where $a = 0$. In this case, the pore is exhausted, so we should expect that $C_p = 1$. However, if we let

$$a(z_p, \tau) = h_T^{-2} \bar{a}(z_p, \tau), \quad (4.5)$$

then (3.4) becomes

$$\frac{\partial^2 C_p}{\partial z_p^2} = k(z) C_p \bar{a}, \quad (4.6)$$

which would seem to imply that the flux in C_p could be $O(1)$, which would then cause an $O(1)$ variation in C . But substituting (4.5) into (3.1), we have

$$h_T^{-1} \frac{\partial \bar{a}}{\partial \tau} = -k(z) C_p \bar{a},$$

which forces $\bar{a} = 0$ as well. Substituting this result into (4.6) and using (3.7), we have that C_p is a constant. From (3.17), we then have that when $a = 0$, C is uniform in z . Because of the boundary condition (3.18), it follows that C must be one in this region.

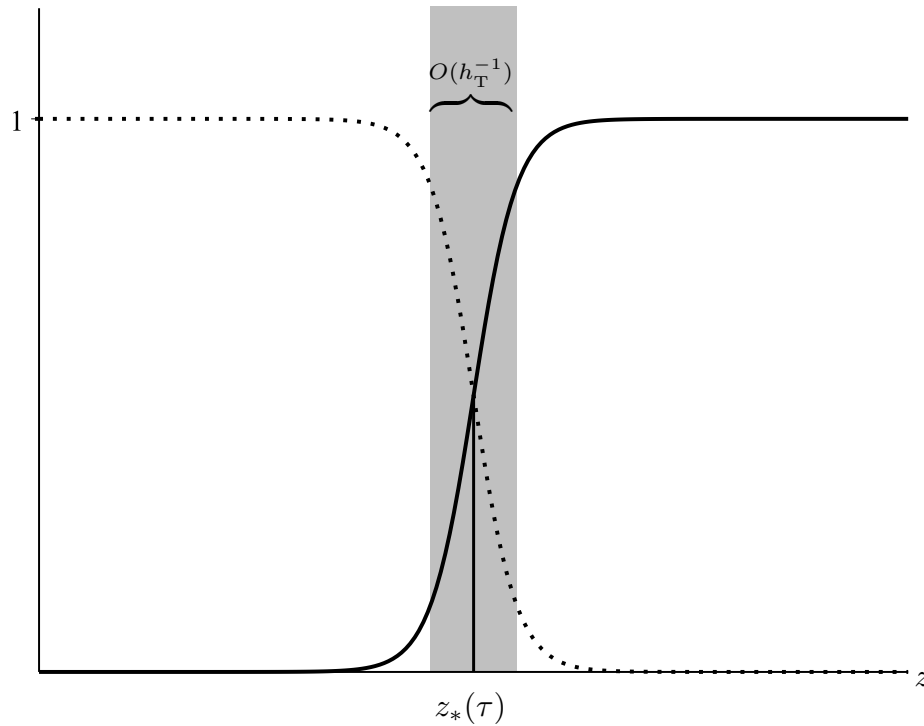


FIGURE 4.1. Schematic of large- h_T solution. Solid line: a . Dotted line: C . $z_*(\tau)$ moves with speed which is $O(h_T^{-1})$.

This discussion is summarized in Fig. 4.1. In the region $0 \leq z \leq z_*(\tau)$, the pores are exhausted ($a = 0$) and the sulfur concentration is saturated ($C = 1$). In the region $z_*(\tau) \leq z \leq 1$, the pores are empty ($a = 1$) and the sulfur concentration is zero to leading order. Then there is a small boundary layer of width $O(h_T^{-1})$ about z_* where both C and a undergo a transition between these extremal values. This front moves on a time scale which is $O(h_T)$, consistent with the observation that fouling occurs on a longer time scale than diffusion.

Returning to dimensional variables, we obtain

$$\tau = \frac{t}{h_T} = \frac{\tilde{t}}{t_k h_T},$$

so the fouling time scale is given by

$$t_k h_T = \left(\frac{1}{C_0 k_0} \right) \frac{R_b}{2} \sqrt{\frac{2k_0 a_{\max}}{D R_p}} = \frac{R_b}{C_0} \sqrt{\frac{a_{\max}}{2k_0 D R_p}}, \quad (4.7)$$

where we have used (3.6).

We now examine the small- h_T limit, which corresponds to the case of very slow reaction compared to transport, which is not seen experimentally. In this case, (3.4) becomes

$$\frac{\partial^2 C_p}{\partial z_p^2} = 0,$$

which we may solve subject to (3.2) and (3.7) to obtain

$$C_p(z_p, t) = C(z, t). \quad (4.8)$$

Hence C_p is uniform in z_p , which is consistent with our interpretation that this case is not diffusion-limited. Substituting this result into (3.17), we have

$$\alpha_2 \frac{\partial C}{\partial z} = 0,$$

so C is independent of z . Then using (3.18), we have that $C = 1$ everywhere, which is consistent with a reaction which isn't fast enough to absorb the sulfur before it transits out of the bed.

For completeness, we make these substitutions in (3.1) to obtain the following:

$$\begin{aligned} \frac{\partial a}{\partial t} &= -k(z)a \\ a(z_p, t) &= e^{-k(z)t}, \end{aligned} \quad (4.9)$$

where we have used (3.8).

Section 5: The “Quasisteady” Case

In order to try to get a handle on the problem analytically, we consider the case when a evolves on a different time scale from C_p . This is motivated by the discussion in [2, §12.3.1]. In that work, a serves merely as a catalytic reaction site; it isn't actually used up by the reaction. Hence $a \equiv 1$ and equation (3.4) is replaced by

$$\frac{\partial^2 C_p}{\partial z_p^2} = h_T^2 k(z) C_p.$$

If a evolves on a much different time scale from C_p , we can separate the scales and treat t [and hence $a(t)$] as a parameter in the evolution equation, as follows:

$$\frac{d^2 C_p}{dz_p^2} = h_T^2 k(z) C a(t). \quad (5.1)$$

Note that we use a total derivative to indicate the separation of scales. Note also that we are assuming that a is independent of z . Solving (5.1) subject to (3.2) and (3.7), we obtain

$$C_p(z_p; t) = C(z, t) \frac{\cosh[h_T(1 - z_p)\sqrt{k(z)a(t)}]}{\cosh[h_T\sqrt{k(z)a(t)}]}. \quad (5.2)$$

Note that C_p may also depend on t parametrically through $C(z, t)$.

This solution can then be used to find an explicit solution for the right-hand side of (3.17): the effective reaction rate within the entire pore, which must balance the flux of sulfur into the pore:

$$\frac{dC_p}{dz_p}(0) = -C(z, t) h_T \sqrt{k(z)a(t)} \tanh[h_T \sqrt{k(z)a(t)}]. \quad (5.3)$$

This expression can be related to the *effectiveness factor* described in the literature (cf. [1, §3.6.1]), which is just (in our notation)

$$\frac{\tanh h_T \sqrt{k(z)a(t)}}{h_T \sqrt{k(z)a(t)}}. \quad (5.4)$$

We can examine our expression (5.3) in two asymptotic limits, though for physical interpretation it is more useful to consider the reaction rate times the cross-sectional area of the pore, which we call the *flux sink per pore*. Writing this quantity in dimensional variables, we obtain the following:

$$\frac{\text{flux sink}}{\text{pore}} = \pi R_p^2 \frac{DC_0}{L_p} \frac{dC_p}{dz_p}(0), \quad (5.5)$$

where we have used (2.4a).

If diffusion is infinitely fast (the *well-mixed* case) or a_{\max} is small, $h_T \rightarrow 0$ and we may use the linear approximation for the tanh to obtain

$$\begin{aligned} \frac{\text{flux sink}}{\text{pore}} &= \pi R_p^2 \frac{DC_0}{L_p} [-C(z, t) h_T^2 k(z) a(t)] = -\pi R_p^2 \frac{D}{L_p} \left(\frac{2k_0 a_{\max} L_p^2}{DR_p} \right) \tilde{C}(\tilde{z}, \tilde{t}) k(z) a(t) \\ &= -(2\pi R_p L_p) \tilde{C}(\tilde{z}, \tilde{t}) \tilde{k}(\tilde{z}) \tilde{a}(\tilde{t}), \end{aligned} \quad (5.6a)$$

where we have used (3.4). Note that in this case, the flux is just the integrated sink over the surface area of the pore.

However, if diffusion is very slow or a_{\max} is very large (the case we expect experimentally), $h_T \rightarrow \infty$, and we may use the constant approximation for the tanh to obtain the following:

$$\begin{aligned} \frac{\text{flux sink}}{\text{pore}} &= \frac{\pi R_p^2 DC_0}{L_p} [-C(z, t) h_T \sqrt{k(z) a(t)}] = -\frac{\pi R_p^2 D}{L_p} \tilde{C}(\tilde{z}, \tilde{t}) \sqrt{\frac{2k_0 a_{\max} L_p^2}{DR_p}} \sqrt{k(z) a(t)} \\ &= -\pi \tilde{C}(\tilde{z}, \tilde{t}) \sqrt{2DR_p^3 \tilde{k}(\tilde{z}) \tilde{a}(\tilde{t})}. \end{aligned} \quad (5.6b)$$

Note that in this case the length of the pore drops out, since diffusion is so slow that only the part of the pore near the opening contributes.

We now want to interpret this flux sink differently. The sulfur molecules removed at the open pore end must be used to decrease a , which is embedded on the surface of the pore. Hence if we treat the pore surface as uniform, we have

$$\pi R_p^2 \frac{DC_0}{L_p} \frac{dC_p}{dz_p}(0) = 2\pi R_p L_p \frac{\partial \tilde{a}}{\partial \tilde{t}}.$$

Substituting our scales from before yields

$$\frac{dC_p}{dz_p}(0) = \frac{2L_p^2}{DC_0 R_p} a_{\max} k C_0 \frac{\partial a}{\partial t} = h_T^2 \frac{\partial a}{\partial t}, \quad (5.7)$$

where we have used (3.4). Substituting (5.7) into (3.17), we obtain

$$\alpha_2 \frac{\partial C}{\partial z} = h_T^2 \frac{\partial a}{\partial t}. \quad (5.8)$$

Substituting (5.7) into (5.3), we have the following:

$$\begin{aligned} h_T^2 \frac{\partial a}{\partial t} &= -C(z, t) h_T \sqrt{ka} \tanh(h_T \sqrt{ka}) \\ C(z, t) &= -h_T \frac{\coth(h_T \sqrt{ka})}{\sqrt{ka}} \frac{\partial a}{\partial t}. \end{aligned} \quad (5.9)$$

Equation (5.9) may be simplified as follows:

$$\begin{aligned}
 -\frac{2}{k} \frac{h_T}{2} \sqrt{\frac{k}{a}} \coth(h_T \sqrt{ka}) \frac{\partial a}{\partial t} &= -\frac{2}{k} \frac{\partial}{\partial t} \left(\log(\sinh(h_T \sqrt{ka})) \right) = C \\
 -\frac{\partial f}{\partial t} &= C, \quad f = \frac{2}{k} \log(\sinh(h_T \sqrt{ka})).
 \end{aligned} \tag{5.10}$$

Initially, there is no sulfur in the system and all the binding sites are free:

$$C(z, 0) = 0, \quad a(z, 0) = 1, \tag{5.11}$$

where in deriving the second condition we recall the scaling on \tilde{a} . Note also that even though we have assumed that a doesn't depend on z_p , it will depend on z through the coupling to the bulk. Using (5.11), we have that

$$f(z, 0) = \frac{2}{k} \log(\sinh(h_T \sqrt{k})). \tag{5.12a}$$

We note from (3.18) and (5.10) that

$$\begin{aligned}
 -\frac{df}{dt}(0, t) &= C(0, t) = 1 \\
 f(0, t) &= \frac{2}{k(0)} \log(\sinh(h_T \sqrt{k(0)})) - t,
 \end{aligned} \tag{5.12b}$$

where we have used (5.12a) to force continuity at the origin.

Continuing to simplify, we have

$$\begin{aligned}
 -\frac{\partial^2 f}{\partial z \partial t} &= \frac{\partial C}{\partial z} = \frac{h_T^2}{\alpha_2} \frac{\partial a}{\partial t} \\
 -\frac{\partial f}{\partial z} &= \frac{h_T^2}{\alpha_2} a + g(z),
 \end{aligned}$$

where we have used (5.8).

At this point, we note that k varies only when the species of porous medium changes. Hence in large portions of the vessel, we can consider it to be a constant. Therefore, for simplicity we now take $\tilde{k}(\tilde{z}) = k_0$, or $k = 1$.

Then using (5.12a), we obtain

$$\begin{aligned}
 -\frac{df}{dz}(z, 0) = 0 &= \frac{h_T^2}{\alpha_2} a(z, 0) + g(z) = \frac{h_T^2}{\alpha_2} + g(z) \\
 -\frac{\partial f}{\partial z} &= \frac{h_T^2(a-1)}{\alpha_2} \\
 \frac{\coth(h_T \sqrt{a})}{h_T \sqrt{a}} \frac{da}{dz} &= \frac{1-a}{\alpha_2},
 \end{aligned} \tag{5.13a}$$

where in the final line we have made explicit the fact that t appears only as a parameter from the boundary condition, which we may obtain from (5.12b):

$$\begin{aligned}
2 \log(\sinh(h_T \sqrt{a(0, t)})) &= 2 \log(\sinh(h_T)) - t \\
\log(\sinh(h_T \sqrt{a(0, t)})) &= \log(\sinh(h_T)) - \frac{t}{2} \\
\sinh(h_T \sqrt{a(0, t)}) &= \sinh(h_T) \exp(-t/2) \\
h_T \sqrt{a(0, t)} &= \sinh^{-1}\left(e^{-t/2} \sinh h_T\right) \\
a(0, t) &= \frac{1}{h_T^2} \left[\sinh^{-1}\left(e^{-t/2} \sinh h_T\right) \right]^2. \tag{5.13b}
\end{aligned}$$

Unfortunately, (5.13) can't be solved explicitly, so we have to do the final step numerically. Then the steps are as follows:

1. Find $a(z, t)$ numerically.
2. Find $f(z, t)$ and $C(z, t)$ using (5.10).
3. Find $C(1, t)$ to find the breakout time where $C(1, t_B) = C_B$. However, this is really just a constant; what we really need to figure out is the dependence on the underlying material and experimental parameters.

Section 6: Asymptotics for Quasisteady Case

We now examine the quasisteady problem analytically in the limits of small and large h_T . In this section, we will take $k(z) = 1$.

We begin with the case of small h_T . In that case, (5.13b) becomes

$$a(0, t) \sim \frac{1}{h_T^2} \left[\sinh^{-1} \left(e^{-t/2} h_T \right) \right]^2 \sim \frac{1}{h_T^2} \left[e^{-t/2} h_T \right]^2 = e^{-t}, \quad (6.1)$$

and (5.13a) becomes

$$\begin{aligned} \frac{1}{(h_T \sqrt{a})^2} \frac{da}{dz} &= \frac{1-a}{\alpha_2} \\ \frac{1}{a(1-a)} \frac{da}{dz} &= \frac{h_T^2}{\alpha_2} \\ \left(\frac{1}{a} - \frac{1}{a-1} \right) \frac{da}{dz} &= \frac{h_T^2}{\alpha_2} \\ \log |a| - \log |a-1| &= \frac{h_T^2 z}{\alpha_2} + b \\ \frac{a}{1-a} &= \frac{e^{-t}}{1-e^{-t}} \exp \left(\frac{h_T^2 z}{\alpha_2} \right), \end{aligned} \quad (6.2)$$

where we have used (6.1). Continuing to simplify, we obtain

$$\begin{aligned} a \left[1 + \frac{e^{-t}}{1-e^{-t}} \exp \left(\frac{h_T^2 z}{\alpha_2} \right) \right] &= \frac{e^{-t}}{1-e^{-t}} \exp \left(\frac{h_T^2 z}{\alpha_2} \right) \\ a(z, t) &= \frac{e^{-t}}{1-e^{-t}} \exp \left(\frac{h_T^2 z}{\alpha_2} \right) \left[1 + \frac{e^{-t}}{1-e^{-t}} \exp \left(\frac{h_T^2 z}{\alpha_2} \right) \right]^{-1} \\ &= \left[\frac{1-e^{-t}}{e^{-t}} \exp \left(-\frac{h_T^2 z}{\alpha_2} \right) + 1 \right]^{-1} \\ &= \left[(e^t - 1) \exp \left(-\frac{h_T^2 z}{\alpha_2} \right) + 1 \right]^{-1}. \end{aligned} \quad (6.3)$$

Note that a is nearly uniform in z in this instance.

Now rewriting (5.10) in this limit, we have

$$\begin{aligned} f &= 2 \log(h_T \sqrt{a}) \\ -\frac{\partial f}{\partial t} &= -\frac{1}{a} \frac{\partial a}{\partial t} = C \end{aligned}$$

$$\begin{aligned}
C(z, t) &= - \left[(e^t - 1) \exp\left(-\frac{h_T^2 z}{\alpha_2}\right) + 1 \right] \times \\
&\quad \left\{ - \left[(e^t - 1) \exp\left(-\frac{h_T^2 z}{\alpha_2}\right) + 1 \right]^{-2} e^t \exp\left(-\frac{h_T^2 z}{\alpha_2}\right) \right\} \\
&= e^t \exp\left(-\frac{h_T^2 z}{\alpha_2}\right) \left[(e^t - 1) \exp\left(-\frac{h_T^2 z}{\alpha_2}\right) + 1 \right]^{-1} \\
&= \left\{ 1 + e^{-t} \left[\exp\left(\frac{h_T^2 z}{\alpha_2}\right) - 1 \right] \right\}^{-1}. \tag{6.4}
\end{aligned}$$

Then using this expression to find t_B , we have

$$\begin{aligned}
[C(1, t_B)]^{-1} &= C_B^{-1} = 1 + e^{-t_B} \left[\exp\left(\frac{h_T^2}{\alpha_2}\right) - 1 \right] \\
\left[\exp\left(\frac{h_T^2}{\alpha_2}\right) - 1 \right]^{-1} (C_B^{-1} - 1) &= e^{-t_B} \\
t_B &= -\log \left((C_B^{-1} - 1) \left[\exp\left(\frac{h_T^2}{\alpha_2}\right) - 1 \right]^{-1} \right) \\
&= \log \left(\frac{1}{C_B^{-1} - 1} \left[\exp\left(\frac{h_T^2}{\alpha_2}\right) - 1 \right] \right). \tag{6.5}
\end{aligned}$$

In the case which we expect ($h_T \rightarrow \infty$), it is easiest to begin with (5.9). For any $a = O(1)$, we have an unacceptably large C . Therefore, shifting to the τ time scale, we have the following:

$$\hat{C} = -\frac{\coth(h_T \sqrt{\hat{a}}) \partial \hat{a}}{\sqrt{\hat{a}} \partial \tau}.$$

We must be careful about expanding this term for large h_T , because the behavior as $\hat{a} \rightarrow 0$ (which is the fouling we are interested in) is much different from the case where $\hat{a} = O(1)$. Continuing, we see that the analog of (5.10) is

$$-\frac{\partial \hat{f}}{\partial \tau} = \hat{C}, \quad \hat{f} = \frac{2}{h_T} \log(\sinh(h_T \sqrt{\hat{a}})). \tag{6.6}$$

Note that $\hat{f} \approx 2\sqrt{\hat{a}}$ if $\hat{a} = O(1)$, since the h_T terms will cancel.

On the other hand, as \hat{a} decreases to zero as the fouling occurs, we would then introduce the variable \bar{a} as defined in (4.5), yielding

$$\hat{f} = \frac{2}{h_T} \log(\sinh(\sqrt{\bar{a}})). \tag{6.7}$$

The boundary conditions are given by

$$\hat{f}(z, 0) = \frac{2}{h_T} \log(\sinh(h_T)) \approx 2, \tag{6.8a}$$

where we use the fact that h_T isn't multiplying anything. We note from (3.18) and (6.6) that

$$\begin{aligned} -\frac{d\hat{f}}{d\tau}(0, \tau) &= \hat{C}(0, \tau) = 1 \\ \hat{f}(0, \tau) &= \frac{2}{h_T} \log(\sinh(h_T)) - \tau \approx 2 - \tau, \end{aligned} \quad (6.8b)$$

where we have used (6.8a) to force continuity at the origin.

Continuing to simplify, we have

$$\begin{aligned} -\frac{\partial^2 \hat{f}}{\partial z \partial \tau} &= \frac{\partial \hat{C}}{\partial z} = \frac{h_T}{\alpha_2} \frac{\partial \hat{a}}{\partial \tau} \\ -\frac{\partial \hat{f}}{\partial z} &= \frac{h_T}{\alpha_2} \hat{a} + g(z), \end{aligned}$$

where we have used the analog of (5.8) in the τ variable. Then using (6.8a) yields

$$\begin{aligned} -\frac{df}{dz}(z, 0) = 0 &= \frac{h_T}{\alpha_2} \hat{a}(z, 0) + g(z) = \frac{h_T^2}{\alpha_2} + g(z) \\ -\frac{\partial \hat{f}}{\partial z} &= \frac{h_T(\hat{a} - 1)}{\alpha_2} \\ \frac{\coth(h_T \sqrt{\hat{a}})}{h_T \sqrt{\hat{a}}} \frac{d\hat{a}}{dz} &= \frac{1 - \hat{a}}{\alpha_2}, \end{aligned} \quad (6.9a)$$

which is exactly analogous to (5.13a). In the final line we have made explicit the fact that t appears only as a parameter from the boundary condition, which we may obtain from (6.8b):

$$\begin{aligned} \frac{2}{h_T} \log(\sinh(h_T \sqrt{\hat{a}(0, \tau)})) &= 2 - \tau \\ \log(\sinh(h_T \sqrt{\hat{a}(0, t)})) &= h_T - \frac{\tau h_T}{2} \\ \sinh(h_T \sqrt{\hat{a}(0, t)}) &= \exp(h_T - t/2) \\ h_T \sqrt{\hat{a}(0, t)} &= \sinh^{-1}(e^{h_T - t/2}) \\ \hat{a}(0, t) &= \frac{1}{h_T^2} \left[\sinh^{-1}(e^{h_T - t/2}) \right]^2. \end{aligned} \quad (6.9b)$$

Now if $\hat{a} = O(1)$, (6.9a) becomes

$$\begin{aligned} \frac{1}{h_T \sqrt{\hat{a}}} \frac{d\hat{a}}{dz} &= \frac{1 - \hat{a}}{\alpha_2} \\ \frac{d\hat{a}}{\sqrt{\hat{a}}(1 - \hat{a})} &= \frac{h_T dz}{\alpha_2} \\ 2 \tanh^{-1} \sqrt{\hat{a}} &= \frac{h_T z}{\alpha_2} + A \\ \sqrt{\hat{a}} &= \tanh \left(\frac{h_T z}{2\alpha_2} + \tanh^{-1} \left(\frac{1}{h_T^2} \left[\sinh^{-1}(e^{h_T - t/2}) \right]^2 \right) \right), \end{aligned} \quad (6.10)$$

where we have used (6.9b). Continuing to simplify, we have

$$\hat{a} = \tanh^2 \left(\frac{h_{\text{T}} z}{2\alpha_2} + \tanh^{-1} \left(\frac{1}{h_{\text{T}}^2} \left[\sinh^{-1} \left(e^{h_{\text{T}} - t/2} \right) \right]^2 \right) \right), \quad (6.11)$$

which has the behavior of a very steep front between $\hat{a}(0, t)$ and 1 due to the $h_{\text{T}} z$ term. Again, we should be able to calculate f (tediously), then \hat{C} .

We conclude with some remarks about the scalings. Even though we didn't always write it down explicitly, from (6.10) there is a typical length scale of $2\alpha_2/h_{\text{T}}$ in the large- h_{T} limit, and from (6.4) there is a typical length scale of α_2/h_{T}^2 in the small- h_{T} limit. These should be investigated further.

Section 7: Conclusions and Further Research

In order to increase the efficiency and lifespan of fuel cells, the feedstock of hydrogen gas must be free of sulfur impurities. Therefore, Bloom Energy has been experimenting with different filtering beds and techniques in order to reduce those impurities. Currently, laboratory results on the efficacy of a particular filtering bed mixture can differ from those in the field. In particular, a mixture that looks promising in the lab can be found in real-world testing to be less effective than current mixtures. However, this real-world testing is expensive and lengthy.

By understanding the underlying physical dynamics, experimentalists can design laboratory protocols that more faithfully replicate real-world conditions. In this work, we have derived and analyzed a model for the desulfurization process in fuel-cell assemblies. We discovered several different time scales on which physical processes occur, and identified the two most important: the t_k time scale given by (2.12), on which individual pores fail, and the τ time scale [in the limit of large Thiele modulus, described in (4.7)], on which the entire device fails.

We found that the underlying dynamics are given by two equations in the pore [(3.1) and (3.4)], which are coupled to the dynamics in the entire bed *via* (3.17). In order for results from the lab and the field to be comparable, the constraint (3.19) must be satisfied. [Interestingly, this constraint involves the convective time scale (2.6), which can also be interpreted as the space velocity.]

In the systems under consideration, there seems to be a distinct separation of scales between the time needed to clog a single pore and the time needed to foul the entire device. This corresponds to the case of large Thiele modulus, and we examined that case in §4. The analysis shows a slowly moving front effecting a sharp transition between a region where the pores are nearly totally fouled, and one where they are nearly totally empty, as shown in Fig. 4.1. These results are borne out by numerical simulations. For completeness, we also discussed the vastly simpler case of small Thiele modulus, which linearizes the system.

We also examined the “quasisteady” case where the number of active sites in the pore is considered to be spatially uniform. In that case, the system can be simplified somewhat, leading to the nonlinear ODE system (5.13), which is easier to solve than the full coupled PDE system. Asymptotics on this case did provide explicit solutions.

In summary, Bloom Energy should ensure that the constraint (3.19) is satisfied when performing their laboratory experiments. (This does not seem to be the case currently.) This should ensure consistency between the laboratory and experimental results.

In the future, a numerical code could be implemented for the PDE system. With good estimates of the relevant parameters for various types of beads, one should be able to perform numerical simulations first. These could then inform the types of bead mixtures to try, thus directing the laboratory experiments to greater effect.

One other facet of the problem we discussed was the placement of the inlet and outlet ports. Currently the inlet port is centered in the bed, while the outlet port is set to one

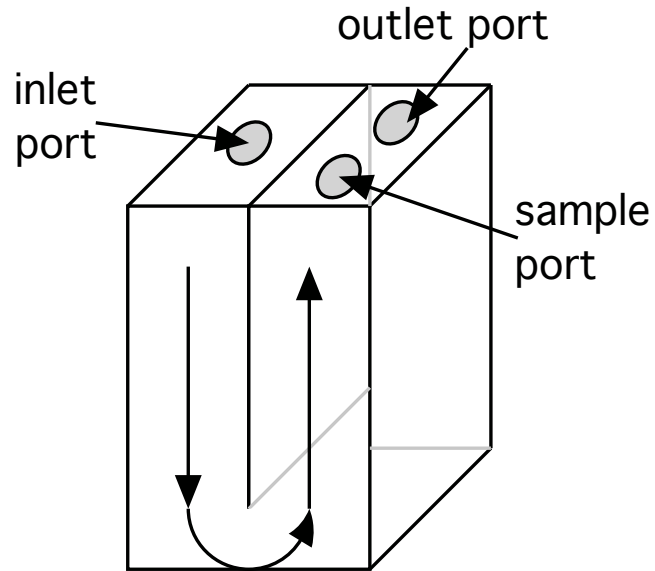


FIGURE 7.1. Representation of bed reactor with ports.

side, since there is a secondary sampling port at that end (see Figure 7.1). Thus, as the gas is diverted to the side of the outlet port, some portion of the filter media under the sample port is underutilized. This could be remedied by moving the outlet port as close to the center as possible, and moving the sample port to the edges of the device. Alternatively, another sampling mechanism (perhaps involving a valve system) could be devised.

Nomenclature

Units are listed in terms of mass (M), moles (N), length (L), time (T), and temperature (θ). If a symbol appears both with and without tildes, the symbol with tildes has units, while the one without is dimensionless. Equation numbers where a variable is first defined is listed, if appropriate.

- \tilde{a} : concentration of active reacting sites, units N/L^2 (2.2).
- b : arbitrary constant, variously defined.
- \tilde{C} : concentration of sulfur, units N/L^3 (1.1).
- D : diffusion coefficient of sulfur in natural gas, units L^2/T (2.1).
- Da: Damköhler number (2.13).
- f : hyperbolic function used for simplification (5.10).
- g : arbitrary function, variously defined.
- H : height of channel, units L .
- h_T : Thiele modulus (3.4).
- $\tilde{k}(\tilde{z})$: association constant, units $L^3/(NT)$ (2.3).
- L : length of channel, units L (1.1).
- M : molecular mass, units M (A.12).
- P : pressure head (A.3).
- Pe: Péclet number (2.8).
- Q : volumetric flow rate, units L^3/T .
- R : radius in pore model.
- \tilde{r} : radial coordinate in pore model (2.1).
- T : temperature, units θ (A.7).
- \tilde{t} : time, units T .
- U : gas velocity, units L/T (2.1).
- V : volume, units L^3 (3.12).
- W : width of channel, units L .
- \tilde{x} : transverse distance, units L .
- \tilde{y} : transverse distance, units L .
- \tilde{z} : distance along the channel, units L .
- α : dimensionless constant in vessel evolution equation (3.16).
- ζ : layer variable (4.1).
- μ : bulk viscosity of natural gas, units $M/(LT)$ (A.9).
- ρ : density of natural gas, units M/L^3 (A.8).
- τ : slow time variable (4.3).
- ϕ : void fraction (3.12).

Other Notation

- B: as a subscript, used to indicate the breakout ratio (1.1).
- b: as a subscript, used to refer to the porous bead (3.5).
- c: as a subscript, used to indicate convection (2.6).
- d: as a subscript, used to indicate diffusion (2.7).
- f: as a subscript, used to indicate a bed used in the field (3.19).
- k: as a subscript, used to indicate reaction (2.12).
- l: as a subscript, used to indicate a bed used in the lab (3.19).
- max: as a subscript on a , used to indicate the maximum number of binding sites available (2.4a).
- p: as a subscript, used to indicate the pore (3.1).
- 0: as a subscript, used to indicate an input value (1.1).
- *: as a subscript, used to indicate a characteristic scale (2.4a) or a front position (4.3).
- $\bar{}$: used to indicate a boundary-layer variable (4.5).
- $\hat{}$: used to indicate a boundary-layer variable (4.1).

References

- [1] G. Froment, K. Bischoff, and J. De Wilde. *Chemical Reactor Analysis and Design, 3rd Edition*. John Wiley & Sons, 2010. URL: <https://books.google.com/books?id=1bQbAAAAQBAJ>.
- [2] C. G. Hill. *An Introduction to Chemical Engineering Kinetics & Reactor Design*. John Wiley & Sons, 1977.
- [3] Hyperphysics. Viscosity of liquids and gases. URL: <http://hyperphysics.phy-astr.gsu.edu/hbase/tables/viscosity.html> [cited July 10, 2015].
- [4] Wolfram. WolframAlpha. URL: <http://www.wolframalpha.com/input/?i=methane+gas+at+25+C+and+2+atm> [cited July 10, 2015].

Appendix: Parameter Values

For our purposes, the field beds may be thought of as having the following dimensions:

$$H_f = 1.15 \times 10^{-1} \text{ m}, \quad W_f = 2.30 \times 10^{-1} \text{ m}, \quad L_f = 2 \text{ m}. \quad (\text{A.1})$$

A typical flow rate in the field is given by

$$Q_f = 600 \frac{\text{L}}{\text{min}} = 10 \frac{10^{-3} \text{ m}^3}{\text{s}} = 10^{-2} \frac{\text{m}^3}{\text{s}}, \quad (\text{A.2})$$

which is created by a pressure head of

$$P_f = 15 \text{ psi} \left(6,895 \frac{\text{N/m}^2}{\text{psi}} \right) = 1.03 \times 10^5 \frac{\text{kg}}{\text{m} \cdot \text{s}^2}. \quad (\text{A.3})$$

This flow rate yields a flow velocity of

$$U_f = \frac{Q_f}{\text{cross-sectional area}} = \frac{10^{-2} \text{ m}^3/\text{s}}{(1.15 \times 10^{-1} \text{ m})(2.30 \times 10^{-1} \text{ m})} = 3.78 \times 10^{-1} \frac{\text{m}}{\text{s}}. \quad (\text{A.4})$$

If we wish to idealize the vessel in the field as a cylinder, we would need

$$\begin{aligned} \pi R_f^2 &= H_f W_f \\ R_f^2 &= \frac{(1.15 \times 10^{-1} \text{ m})(2.30 \times 10^{-1} \text{ m})}{3.14} = 0.842 \times 10^{-2} \text{ m}^2 \\ R_f &= 9.18 \times 10^{-2} \text{ m}. \end{aligned} \quad (\text{A.5})$$

In the lab, the bed is cylindrical, so we have

$$\begin{aligned} 0.75 \text{ in} &\leq R_l \leq 1 \text{ in} \\ 1.9 \times 10^{-2} \text{ m} &\leq R_l \leq 2.54 \times 10^{-2} \text{ m}, \end{aligned} \quad (\text{A.6a})$$

$$\begin{aligned} 5 \text{ in} &\leq L_l \leq 21 \text{ in} \\ 1.27 \times 10^{-1} \text{ m} &\leq L_l \leq 5.33 \times 10^{-1} \text{ m}. \end{aligned} \quad (\text{A.6b})$$

The temperature of the experiment is room temperature, which we take to be

$$T = (273 + 25) \text{ K} = 298 \text{ K}. \quad (\text{A.7})$$

To calculate the Reynolds number, we first write down the density of methane (natural gas) [4] at 298 K:

$$\rho = 1.316 \frac{\text{kg}}{\text{m}^3}. \quad (\text{A.8})$$

We also need the viscosity [3]:

$$\mu = 2 \times 10^{-4} \text{ poise} = 2 \times 10^{-5} \text{ Pa} \cdot \text{s} = 2 \times 10^{-5} \frac{\text{kg}}{\text{m} \cdot \text{s}}. \quad (\text{A.9})$$

With these measurements, we may calculate a typical Reynolds number for the system:

$$\begin{aligned} \text{Re} &= \frac{\rho U_f R_f}{\mu} = \left(1.316 \frac{\text{kg}}{\text{m}^3}\right) \left(3.78 \times 10^{-1} \frac{\text{m}}{\text{s}}\right) (9.18 \times 10^{-2} \text{ m}) \left(2 \times 10^{-5} \frac{\text{kg}}{\text{m} \cdot \text{s}}\right)^{-1} \\ &= 2.28 \times 10^3. \end{aligned} \quad (\text{A.10})$$

The Knudsen diffusivity for a gas is given by [2, (12.2.4)]:

$$D = 9.7 \times 10^3 R_p \sqrt{\frac{T}{M}} \frac{\text{cm} \cdot \text{g}^{1/2}}{\text{s} \cdot \text{K}^{1/2} \cdot \text{mol}^{1/2}}, \quad (\text{A.11})$$

where T is the temperature and M is the molecular weight of the gas. The molecular weight of two of the sulfur-carrying gases we are interested in (THT and TBM) are

$$M = 90 \frac{\text{g}}{\text{mol}}. \quad (\text{A.12})$$

A typical radius of the pore is given by

$$1 \times 10^{-9} \text{ m} \leq R_p \leq 3 \times 10^{-8} \text{ m}. \quad (\text{A.13})$$

Using the low end of this range, we have

$$\begin{aligned} D &= 9.7 \times 10^3 (10^{-9} \text{ m}) \sqrt{\frac{298 \text{ K}}{90 \text{ g/mol}} \frac{10^{-2} \text{ m} \cdot \text{g}^{1/2}}{\text{s} \cdot \text{K}^{1/2} \cdot \text{mol}^{1/2}}} = 9.7 \times 10^{-8} \sqrt{3.31} \frac{\text{m}^2}{\text{s}} \\ &= 1.77 \times 10^{-7} \frac{\text{m}^2}{\text{s}}. \end{aligned} \quad (\text{A.14})$$

A typical void fraction of the beads is

$$\phi_b = \frac{3}{8}, \quad (\text{A.15a})$$

while a typical void fraction of the pores is

$$\phi_p = 0.4. \quad (\text{A.15b})$$

A typical radius of the bead is given by

$$R_b = 0.8 \text{ mm} = 8 \times 10^{-4} \text{ m}. \quad (\text{A.16})$$

With these values, we may now compute α_2 :

$$\alpha_2 = \frac{(3.78 \times 10^{-1} \text{ m/s})(8 \times 10^{-4} \text{ m})^2}{4(1.77 \times 10^{-7} \text{ m}^2/\text{s})(0.4)(5/8)(2 \text{ m})} = \frac{242 \times 10^{-9}}{3.54 \times 10^{-7}} = 6.83 \times 10^{-1}. \quad (\text{A.17})$$

Hence we may now calculate the Péclet number from (2.8), which we do with the midpoint of the range:

$$\text{Pe}_f = \frac{(3.78 \times 10^{-1} \text{ m/s})/(2 \text{ m})}{(5 \times 10^{-5} \text{ m}^2/\text{s})/(9.18 \times 10^{-2} \text{ m})^2} = \frac{1.89 \times 10^{-1} \text{ s}^{-1}}{(5.93 \times 10^{-2})(10^{-1} \text{ s}^{-1})} = 31.9. \quad (\text{A.18})$$

A typical amount of surface area on a porous bead (expressed in area per mass of bead) is on the order of $1000 \text{ m}^2/\text{g}$.

Integro-differential Formulation

Brooks Emerick
Trinity College

David Rumschitzki
City College of New York

1 Introduction

Let $\tilde{c} = \tilde{c}(\tilde{z}, \tilde{Z}, \tilde{t})$ be the dimensional concentration of sulfur inside a cylindrical pore at position \tilde{z} at level \tilde{Z} within the tank at time \tilde{t} . Let $\tilde{c}_0(\tilde{Z}, \tilde{t}) = \tilde{c}(0, \tilde{Z}, \tilde{t})$ be the concentration of sulfur at the opening of a pellet's pore at level \tilde{Z} within the tank at time \tilde{t} . Finally, let $\tilde{a}(\tilde{z}, \tilde{Z}, \tilde{t})$ be the number of free binding sites inside a pore at position \tilde{z} at level \tilde{Z} inside the tank at time \tilde{t} . It is apparent that there are three timescales associated with the problem:

- The **pore timescale** (0.1 seconds) is associated with $\tilde{t}_p = L_p^2/D$, where L_p is the length of the pore and D is the Knudsen diffusivity of the gas. Dimensions: $[L_p] = L$, $[D] = L^2T^{-1}$.
- The **gas timescale** (10 seconds) is associated with $\tilde{t}_g = L_t/u$, where L_t is the length of the tank and u is the speed at which the gas is flowing through the tank. Dimensions: $[L_t] = L$, $[u] = LT^{-1}$.
- The **fouling timescale** (months) is associated with the timescale $\tilde{t}_f = 1/kc_i$, where k is the rate of binding per unit area and c_i is the initial inlet concentration of sulfur. Dimensions: $[k] = L^3M^{-1}T^{-1}$, $[c_i] = L^{-3}M$.

We simplify the governing equations by taking advantage of the fact that $\tilde{t}_p \ll \tilde{t}_g \ll \tilde{t}_f$ as well as making reasonable assumptions about the pore scale. Below, we consider the dynamics at each level of the problem in dimensional form.

2 Governing Equations

The problem can be broken down into three components: pore-level dynamics, the dynamics of the gas passing through the tank, and the absorption dynamics related to the fouling of filter material.

Pore-Level Dynamics

Let \tilde{Z} and \tilde{t} be fixed and let \tilde{z} vary along the length of the cylindrical hole in the pore, $0 < \tilde{z} < L_p$. The sulfur concentration inside the pore evolves according to the following reaction-diffusion equation:

$$\frac{\partial \tilde{c}}{\partial \tilde{t}} = D \frac{\partial^2 \tilde{c}}{\partial \tilde{z}^2} - \frac{2k}{r} \tilde{a} \tilde{c}$$

subject to the conditions

$$\tilde{c}(\tilde{z}, \tilde{Z}, 0) = 0, \quad \text{and} \quad \tilde{c}(0, \tilde{Z}, \tilde{t}) = \tilde{c}_0, \quad \frac{\partial \tilde{c}}{\partial \tilde{z}}(L_p, \tilde{Z}, \tilde{t}) = 0.$$

Here, D is the diffusivity of the sulfur compound in the gas, k is the rate at which the sulfur clings to free binding sites within the pore per unit area, $\tilde{a} = \tilde{a}(\tilde{z}, \tilde{Z}, \tilde{t})$ is the number of free binding sites within the pores at level \tilde{Z} , and r is the radius of the cylindrical shape of the hole in the pellet. The factor $2/r$ is the surface area per unit volume of the cylindrical pore. The boundary condition at the entrance to the pore is prescribed as an initial concentration \tilde{c}_0 and there is no change in sulfur concentration at the end of the pore. (Note: the boundary condition maintains a “ \sim ” notation as this is a dimensional variable along \tilde{Z} and will be scaled in the next section.) Dimensions:

$$[D] = L^2 T^{-1}, \quad [k] = L^3 M^{-1} T^{-1}, \quad [r] = L, \quad [\tilde{c}_0] = L^{-3} M, \quad [a_0] = L^{-2} M.$$

We nondimensionalize this equation using the following scalings:

$$c = \frac{\tilde{c}}{c_i}, \quad a = \frac{\tilde{a}}{a_0}, \quad z = \frac{\tilde{z}}{L_p}, \quad t_p = \frac{\tilde{t}}{L_p^2} = \frac{D}{L_p^2} \tilde{t}.$$

Here, a_0 is the maximum number of binding sites per pore. Substituting, we obtain the following:

$$\boxed{\frac{\partial c}{\partial t_p} = \frac{\partial^2 c}{\partial z^2} - \phi^2 a c} \tag{1}$$

subject to

$$c(z, Z, 0) = 0, \quad \text{and} \quad c(0, \tilde{Z}, t_p) = \frac{\tilde{c}_0}{c_i}, \quad \frac{\partial c}{\partial z}(1, \tilde{Z}, t_p) = 0.$$

Here, the single nondimensional term ϕ is given by

$$\phi = L_p \sqrt{\frac{2ka_0}{rD}}.$$

ϕ is known as the *Thiele Modulus*. ϕ^2 is the ratio of the characteristic rates of reaction to diffusion in the pore. We note that the number of free binding sites, a , evolves over the longest timescale.

Fouling Dynamics

We now consider the number of free binding sites within a pore of a single pellet. This is given by the function $\tilde{a}(\tilde{z}, \tilde{Z}, \tilde{t})$ and is governed by the following differential equation,

$$\frac{\partial \tilde{a}}{\partial \tilde{t}} = -kac,$$

subject to the following initial condition

$$\tilde{a}(\tilde{z}, \tilde{Z}, 0) = a_0.$$

All variables and parameters are defined with dimensions given above. We nondimensionalize these equations according to the following scalings:

$$a = \frac{\tilde{a}}{a_0}, \quad c = \frac{\tilde{c}}{c_i}, \quad z = \frac{\tilde{z}}{L_p}, \quad t_f = \frac{\tilde{t}}{t_f} = kc_i \tilde{t}.$$

Substituting these scalings into our equation gives the following dimensionless equation:

$$\boxed{\frac{\partial a}{\partial t_f} = -ac} \quad (2)$$

with the initial condition given as

$$a(z, Z, 0) = 1.$$

Gas-Level Dynamics

Finally we consider the concentration of sulfur that is available to every pore in the system within the entire tank. In this sense, we consider the evolution of $\tilde{c}(0, \tilde{Z}, \tilde{t})$, which we will denote by $\tilde{c}_0(\tilde{Z}, \tilde{t})$. The variable \tilde{Z} varies over the length of the tank, $0 < \tilde{Z} < L_t$. This sulfur concentration is advected with the gas velocity that passes through the tank but is taken up by the pellets within the tank whose pores become saturated according to the pore-level dynamics above. Therefore, we have the following transport equation for \tilde{c}_0 :

$$\frac{\partial \tilde{c}_0}{\partial \tilde{t}} + u \frac{\partial \tilde{c}_0}{\partial \tilde{Z}} = \left[D \frac{\partial \tilde{c}}{\partial \tilde{z}} \Big|_{\tilde{z}=0} \right] \frac{\pi r^2}{2\pi r L} \mathcal{A} = -k \mathcal{A} \int_0^{L_p} \tilde{a} \tilde{c} d\tilde{z} - \int_0^{L_p} \frac{\partial \tilde{c}}{\partial \tilde{t}} d\tilde{z},$$

where the second equals sign substitutes the integral of the pore-level equation. This equation is subject to the condition

$$\tilde{c}_0(0, \tilde{t}) = c_i.$$

Here, u is the gas velocity through the tank (assumed to be constant), k is the binding reaction rate constant inside the pore, \mathcal{A} is the reactive surface area per unit volume of the tank, the integral on the right gives the homogenized total rate of reaction within a single pore, and c_i is the initial inlet concentration of sulfur into the tank. Dimensions:

$$[u] = LT^{-1}, \quad [\mathcal{A}] = L^{-1}, \quad [k] = L^3 M^{-1} T^{-1}, \quad [c_i] = L^{-3} M.$$

We nondimensionalize this equation with the following scalings:

$$c = \frac{\tilde{c}}{c_i}, \quad c_0 = \frac{\tilde{c}_0}{c_i}, \quad a = \frac{\tilde{a}}{a_0}, \quad z = \frac{\tilde{z}}{L_p}, \quad Z = \frac{\tilde{Z}}{L_t}, \quad t_g = \frac{\tilde{t}}{\tilde{t}_g} = \frac{u}{L_t} \tilde{t}.$$

Substituting, we obtain the following dimensionless equation

$$\boxed{\frac{\partial c_0}{\partial t_g} + \frac{\partial c_0}{\partial Z} = -\kappa \int_0^1 ac dz - \int_0^1 \frac{\partial c}{\partial t_g} dz} \quad (3)$$

subject to the following condition

$$c_0(0, t_g) = 1.$$

Here, the nondimensional parameter, κ , is given by

$$\kappa = \frac{k \mathcal{A} a_0 L_t}{u} = \frac{\mathcal{A} a_0 \tilde{t}_g}{c_i \tilde{t}_f}.$$

Summary

Equations (1) – (3), given below in their respective timescales, describe the entire system:

$$\begin{aligned} \frac{\partial c}{\partial t_p} &= \frac{\partial^2 c}{\partial z^2} - \phi^2 ac, \\ \frac{\partial c_0}{\partial t_g} + \frac{\partial c_0}{\partial Z} &= -\kappa \int_0^1 ac dz - \int_0^1 \frac{\partial c}{\partial t_g} dz, \\ \frac{\partial a}{\partial t_f} &= -ac. \end{aligned}$$

Asymptotic Simplification

We assemble Equations (1) – (3) and write every equation on the long timescale, t_f , to obtain the following:

$$\begin{aligned} \frac{\tilde{t}_p}{\tilde{t}_f} \frac{\partial c}{\partial t_f} &= \frac{\partial^2 c}{\partial z^2} - \phi^2 ac, \\ \frac{\tilde{t}_g}{\tilde{t}_f} \frac{\partial c_0}{\partial t_f} + \frac{\partial c_0}{\partial Z} &= -\kappa \int_0^1 ac dz - \frac{\tilde{t}_g}{\tilde{t}_f} \int_0^1 \frac{\partial c}{\partial t_f} dz, \\ \frac{\partial a}{\partial t_f} &= -ac. \end{aligned}$$

As noted in the introduction, we know from the characteristics of the system that $\tilde{t}_p \ll \tilde{t}_g \ll \tilde{t}_f$, which means

$$\frac{\tilde{t}_p}{\tilde{t}_f} \ll 1, \quad \frac{\tilde{t}_g}{\tilde{t}_f} \ll 1.$$

For the equation describing the evolution of sulfur concentration inside the local pore, c , we can eliminate the time derivative. Likewise, we can eliminate the time derivative in the equation for c_0 . This gives the concentration of sulfur within the pore and along the tank as a quasi-steady state. Our equations can be updated to the following system on the long timescale:

$$\frac{\partial^2 c}{\partial z^2} = \phi^2 ac, \quad (4)$$

$$\frac{\partial c_0}{\partial Z} = -\kappa \int_0^1 ac dz, \quad (5)$$

$$\frac{\partial a}{\partial t_f} = -ac. \quad (6)$$

3 Simplified Special Case

Since the length scale of a pore (\tilde{z}) inside a pellet is on the order of millimeters and that of the reactor (\tilde{Z}), the scale of interest for sulfur adsorption, is meters, we simplify the problem by neglecting the variation of the number of free receptors along the pore. This leaves a simpler, time-dependent, pore-average (uniform, *i.e.*, averaged, with respect to \tilde{z}) concentration of free binding sites, $\tilde{a}(\tilde{Z}, \tilde{t})$.

With this assumption, we can update Equations (4) – (6) in the following manner. Since a is no longer a function of z , we can find an explicit solution for c in Equation (4) as

$$c(z, Z, t_f) = \frac{c_0}{c_i} \frac{\cosh [\phi\sqrt{a}(1-z)]}{\cosh [\phi\sqrt{a}]},$$

where we have applied the appropriate boundary conditions. For Equation (6), we can integrate over the z dimension to obtain the following equation

$$\frac{\partial a}{\partial t_f} = -a \int_0^1 c dz.$$

To further simplify our equations, we can introduce the *effectiveness factor*, which is the ratio of the true total reaction rate in the pore to that which would hold if diffusion were fast, *i.e.*, if the gas concentration were equal to \tilde{c}_0 everywhere in the pore. This is easily found to be

$$\eta = \eta(a) = \frac{\tanh(\phi\sqrt{a})}{\phi\sqrt{a}},$$

in the case for a cylindrical-shaped pore with uniform a . This factor allows us to replace the integrated rate of loss of free sites average value (by the accumulation of sulfur compounds on them) over the entire pore with $ac_0\eta(a)$ at every point along the tank, *i.e.*,

$$\int_0^1 ac dz = a\eta(a)c_0.$$

This follows from the definition of the effectiveness factor. With these assumptions, our equations can be updated to the following:

$$\frac{\partial^2 c}{\partial z^2} = \phi^2 a c, \quad (7)$$

$$\frac{\partial c_0}{\partial Z} = -\kappa a \eta(a) c_0, \quad (8)$$

$$\frac{\partial a}{\partial t_f} = -a \eta(a) c_0. \quad (9)$$

As mentioned previously, an explicit solution for c exists and we can find an expression for c_0 as

$$c_0(Z, t_f) = \exp \left[-\kappa \int_0^Z a(\xi, t_f) \eta(a(\xi, t_f)) d\xi \right].$$

The system now collapses to the following single differential equation in the free binding sites, a , which evolves over the longest timescale:

$$\boxed{\frac{\partial a}{\partial t_f} = -a \eta(a) \exp \left[-\kappa \int_0^Z a(\xi, t_f) \eta(a(\xi, t_f)) d\xi \right]} \quad (10)$$

with the initial condition $a(Z, 0) = 1$.

Homogenization of Flow Equations over Pore Scale

Chris Breward
Oxford

Richard O. Moore
NJIT

Chris Raymond
University of Delaware

1 Pore equations

Within each pore, the volumetric concentration $C_p(z, t)$ of sulfur molecules and surface concentration $B(z, t)$ of reactive sites (both nondimensionalized) evolve according to

$$\frac{\partial B}{\partial t} = C_p(1 - B), \quad (1)$$

$$\frac{\partial^2 C_p}{\partial z^2} = h_T^2 C_p(1 - B), \quad (2)$$

with boundary conditions $C_p(z, t) = C(x, t)$ (where x is simply a parameter for the purposes of the pore equations), $\frac{\partial C_p}{\partial z}(1, t) = 0$ and initial condition $B(z, 0) = 0$. The objective is to obtain $\frac{\partial C_p}{\partial z}(0, t)$ as a function of $C(x, t)$.

Letting $u = \ln(1 - B)$, we note that $u_t = -C_p$. Substituting and integrating in t produces

$$u_{zz} = h_T^2 e^u + f(z), \quad (3)$$

where $f(z)$ is arbitrary. This is associated with initial condition $u(z, 0) \equiv 0$ and boundary conditions

$$\begin{aligned} \frac{\partial u}{\partial t}(0, t) &= -C(x, t), \\ \frac{\partial^2 u}{\partial z \partial t}(1, t) &= 0. \end{aligned}$$

Application of the initial condition shows that $f(z) \equiv -h_T^2$, and multiplying by u_z allows a first integral yielding

$$\frac{1}{2} u_z^2 = h_T^2 (e^u - u) + g(t) \quad (4)$$

where $g(t)$ is arbitrary. Application of the boundary conditions then gives

$$\frac{1}{2}(u_z^2(1, t) - u_z^2(0, t)) = h_T^2(e^{u(1, t)} - u(1, t) - e^{u(0, t)} + u(0, t)). \quad (5)$$

By combining the initial and boundary conditions we obtain additional conditions $u_z(1, t) = 0$ and $u(0, t) = -\int_0^t C(x, s) ds$. This allows us to write

$$u_z^2(0, t) = 2h_T^2 [e^{u(0, t)} - e^{u(1, t)} - u(0, t) + u(1, t)]. \quad (6)$$

The objective is to obtain $u_{zt}(0, t)$, but we are confronted with the fact that $u(1, t)$ is unknown.

To understand this a little better it is informative to consider the limit of small u (*i.e.*, $B \ll 1$). Then,

$$u_{zz} = h_T^2(e^u - 1) \approx h_T^2 u, \quad (7)$$

which solves to give

$$u(z, t) = a(t) \cosh h_T(1 - z) + b(t) \sinh h_T(1 - z). \quad (8)$$

Applying the initial condition gives $a(0) = b(0) = 0$. Applying the boundary conditions then gives $b(t) \equiv 0$ and

$$a(t) = -\frac{\int_0^t C(x, s) ds}{\cosh h_T}, \quad \text{i.e.,} \quad u(z, t) = -\int_0^t C(x, s) ds \frac{\cosh h_T(1 - z)}{\cosh h_T}, \quad (9)$$

providing the known limiting solution of

$$\frac{\partial C_p}{\partial z} \Big|_{z=0} = -h_T C(x, t) \tanh h_T. \quad (10)$$

The various terms in (6) are:

$$\begin{aligned} u_z(0, t) &= h_T \int_0^t C(x, s) ds \tanh h_T, \\ u(0, t) &= -\int_0^t C(s) ds, \\ u(1, t) &= \frac{-\int_0^t C(x, s) ds}{\cosh h_T}. \end{aligned}$$

Note in particular that in the limit $h_T \gg 1$, $u(1, t)$ is negligible.

Motivated by this limit, we return to Eqn. (6) and set $u(1, t) \approx 0$. Then, noting that we expect $u_z(0, t) > 0$, we have

$$u_z(0, t) \approx \sqrt{2}h_T \sqrt{e^{-\int_0^t C(x, s) ds} + \int_0^t C(x, s) ds} - 1. \quad (11)$$

The radicand is positive definite. Finally, differentiating this with respect to t gives a Dirichlet-to-Neumann flux mapping of

$$\frac{\partial C_p}{\partial z}(0, t) = -u_{zt}(0, t) \approx -\frac{h_T}{\sqrt{2}} \frac{\left(1 - e^{-\int_0^t C(x, s) ds}\right) C(x, t)}{\sqrt{e^{-\int_0^t C(x, s) ds} + \int_0^t C(x, s) ds - 1}}. \quad (12)$$

This quantity obviates the need to compute the microscopic pore model, formally in the limit of large Thiele modulus h_T .

As a final comparison, we note that in the limit $C \ll 1$ (and therefore $|u| \ll 1$), this expression collapses to

$$\frac{\partial C_p}{\partial z}(0, t) = -h_T C(x, t), \quad (13)$$

which agrees with Eqn. (10) in the appropriate limit of large h_T .

2 Channel equations

We now couple Eqn. (12) to convection in the channel by posing the aggregate flux into pores at each value of x and t as a sink, *i.e.*,

$$\frac{\partial C}{\partial t} + U \frac{\partial C}{\partial x} = -\frac{\beta h_T}{\sqrt{2}} \frac{\left(1 - e^{-\int_0^t C(x, s) ds}\right) C(x, t)}{\sqrt{e^{-\int_0^t C(x, s) ds} + \int_0^t C(x, s) ds - 1}}, \quad (14)$$

where U is the average fluid velocity in the channel and β is a scaling constant accounting for the volumetric pore density. This equation is accompanied by conditions $C(x, 0) = 0$ and $C(0, t) = C_0$.

We assume that temporal variations of C on the scale of the channel length are small (*i.e.*, dimensionless u is large). Making this assumption and converting the integro-differential equation into a coupled system through $C = \partial\Gamma/\partial t$, we have

$$\begin{aligned} \Gamma_t &= C, \\ C_x &= -\alpha \frac{(1 - e^{-\Gamma})C}{\sqrt{e^{-\Gamma} + \Gamma - 1}}, \end{aligned}$$

accompanied by initial/boundary conditions $\Gamma(x, 0) = 0$ and $C(0, t) = 1$, where

$$\alpha = \frac{\beta h_T}{\sqrt{2}U} \quad (15)$$

is a dimensionless parameter characterizing the (inverse) length of the “mass-transfer zone” in the channel.

These equations are combined to give

$$\Gamma_{tx} = -\alpha \frac{(1 - e^{-\Gamma})\Gamma_t}{\sqrt{e^{-\Gamma} + \Gamma - 1}}, \quad (16)$$

which can be integrated in time and combined with $\Gamma(x, 0) = 0$ to give

$$\Gamma_x = -2\alpha\sqrt{e^{-\Gamma} + \Gamma - 1}. \quad (17)$$

Thus, the dynamics of pore and channel are effectively reduced to a single ordinary differential equation, parameterized by time, with boundary condition

$$\Gamma(0, t) = t. \quad (18)$$

Once $\Gamma(x, t)$ is computed, the concentration is recovered through

$$C(x, t) = \Gamma_t. \quad (19)$$

3 Computations and limits

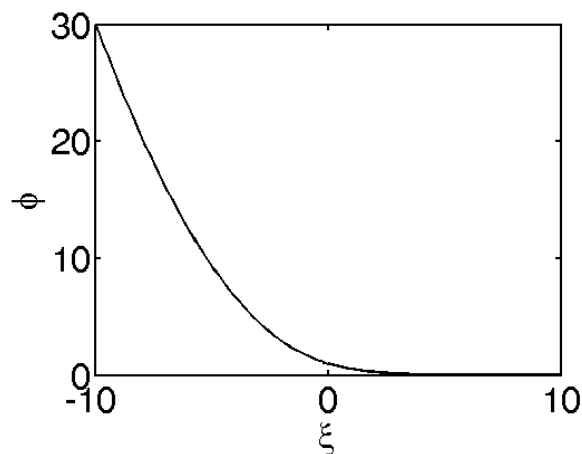
Let $\phi(\xi)$ be the unique solution of

$$\phi'(\xi) = -\sqrt{e^{-\phi} + \phi - 1}, \quad \phi(0) = 1, \quad (20)$$

plotted in Fig. 3. Since ϕ is monotonic, its inverse is well-defined on \mathbb{R}^+ . All solutions of (17) can be expressed using a lookup table for ϕ , *i.e.*,

$$\Gamma(x, t) = \phi(\phi^{-1}(t) + 2\alpha x). \quad (21)$$

The concentration is then expressed by



$$C(x, t) = \frac{\phi'(\phi^{-1}(t) + 2\alpha x)}{\phi'(\phi^{-1}(t))}. \quad (22)$$

The limiting cases of large and small Γ are clear from Eqn. 20. If $\phi \ll 1$, we have

$$\phi' \approx -\frac{\phi}{\sqrt{2}}, \quad (23)$$

so that ϕ decays exponentially,

$$\phi = \phi_0 e^{-\xi/\sqrt{2}}. \quad (24)$$

At the other extreme of $\phi \gg 1$, we have

$$\phi' \approx -\sqrt{\phi}, \quad (25)$$

so that ϕ decays algebraically,

$$\phi = \left(\sqrt{\phi_0} - \frac{1}{2}\xi\right)^2. \quad (26)$$

4 Consistency

As a final note, we recall that the above analysis was motivated by letting $h_T \ll 1$ in the linear limit. It would be nice to have this analysis hold regardless of the size of B ; however, setting $h_T = 0$ in Eqns. 2 forces $C_p(z, t) \equiv C(x, t)$, so that u is approximately uniform in z . This invalidates the assumption that we can neglect $u(1, t)$ in Eqn. (6) relative to $u(0, t)$ and suggests that more careful asymptotics in terms of the order of B should be considered.

Numerical Simulations

D. W. Schwendeman
Rensselær Polytechnic Institute

1 DWS Notes

The purpose of these notes is to describe the numerical approach and simulation results for a mathematical model of gas desulfurization in a packed bed. The description of the mathematical model is brief as details of its derivation are given elsewhere.

1.1 Model

Let us consider a one-dimensional gas flow in a packed bed of length L and cross-sectional area A . The concentration of sulfur in the gas is taken to be $S(x, t)$, where x measures distance down the bed and t is time. It is assumed that the pellets packing the bed are porous and that the sulfur in the gas may diffuse into the pores where it is absorbed onto the surface of the pores. Let $C(x, z, t)$ denote the concentration of sulfur in the pores of the pellets (assumed to be a densely packed continuum), where z measures distance down the pores from the outer surface of the pellets at $z = 0$. Assuming a quasi-steady flow in the bed with constant volume flow rate Q , conservation of mass of the sulfur gives

$$Q \frac{\partial S}{\partial x} = -AN\sigma J(x, z, t)|_{z=0}, \quad 0 < x < L, \quad t > 0, \quad (1)$$

where N is number of pellets per unit volume, σ is the surface area of holes per pellet, and J is the flux of sulfur in the pores of the pellets. Ficks law of diffusion gives

$$J = -D \frac{\partial C}{\partial z}, \quad (2)$$

where D is the diffusivity.

The transport of sulfur in the pores of the pellets (at any position x along the bed) is assumed to be a balance of diffusion along the length of the pores and reaction to the surface of the pores. Modeling the pores as cylindrical tubes of radius R gives

$$\pi R^2 \frac{\partial J}{\partial z} = -2\pi R K C, \quad 0 < x < L, \quad 0 < z < a, \quad t > 0, \quad (3)$$

where \mathcal{K} is the surface reaction rate and a is the length of the cylindrical pore. Using a simple first-order law of mass action, we have

$$\mathcal{K} = kC(B_\infty - B), \quad (4)$$

where k is a rate constant, $B(x, z, t)$ is the concentration of sulfur on the surface of the pore, and B_∞ is the saturation concentration. The concentration of sulfur on the surface of the pore is governed by

$$\frac{\partial B}{\partial t} = \mathcal{K}, \quad 0 < x < L, \quad 0 < z < a, \quad t > 0. \quad (5)$$

The set of model equations given by (1), (3) and (5) require initial conditions and boundary conditions. We assume that the sulfur concentration is known at the inlet of the bed, and take

$$S(0, t) = S_{\text{in}}, \quad t > 0,$$

where S_{in} is the inlet concentration. (The inlet concentration can be a function of time, but we assume that it is constant.) The equation for the transport of the sulfur in the pores requires boundary conditions at $z = 0$ and $z = a$. We assume that the sulfur concentration is continuous at $z = 0$ and no-flux at $z = a$, i.e.

$$C(x, 0, t) = S(x, t), \quad J(x, a, t) = 0, \quad 0 < x < L, \quad t > 0.$$

Finally, the equation for the surface reaction requires an initial condition. We assume that pellets are free of sulfur initially so that

$$B(x, z, 0) = 0, \quad 0 < x < L, \quad 0 < z < a.$$

The model equations can be made dimensionless by choosing suitable reference scales for the various independent and dependent variables. We set

$$x' = \frac{x}{L}, \quad z' = \frac{z}{a}, \quad t' = \frac{t}{t_{\text{ref}}},$$

where the primes denote dimensionless quantities and the reference time scale is taken to be

$$t_{\text{ref}} = t_{\text{rxn}} = \frac{1}{kS_{\text{in}}}, \quad (6)$$

which is the time scale for reaction to the surface of the pores. Dimensionless concentrations are defined by

$$S' = \frac{S}{S_{\text{in}}}, \quad C' = \frac{C}{S_{\text{in}}}, \quad B' = \frac{B}{B_\infty}.$$

Substituting the dimensionless quantities into the set of model equations, simplifying and dropping primes, gives

$$\frac{\partial S}{\partial x} = \alpha \left. \frac{\partial C}{\partial z} \right|_{z=0}, \quad 0 < x < 1, \quad t > 0, \quad (7)$$

along the bed, and

$$\left. \begin{aligned} \frac{\partial^2 C}{\partial z^2} &= \beta C(1 - B) \\ \frac{\partial B}{\partial t} &= C(1 - B) \end{aligned} \right\}, \quad 0 < x < 1, \quad 0 < z < 1, \quad t > 0, \quad (8)$$

in the pores. The dimensionless parameters, α and β , are given by

$$\alpha = \frac{ALN\sigma D}{aQ}, \quad \beta = \frac{2ka^2 B_\infty}{RD}, \quad (9)$$

and the initial and boundary conditions become

$$S(0, t) = 1, \quad C(x, 0, t) = S(x, t), \quad \frac{\partial C}{\partial z}(x, 1, t) = 0, \quad B(x, z, 0) = 0. \quad (10)$$

The two dimensionless parameters can be interpreted in terms of ratios of time scales, and the ratios of certain volumes and masses. Define

$$t_{\text{bed}} = \frac{AL}{Q} = \text{resident time for the gas in the bed,}$$

$$t_{\text{diff}} = \frac{a^2}{D} = \text{time scale for diffusion in the pores,}$$

and let

$$\theta = N\sigma a = \text{ratio of the volume of pores to that of the bed,}$$

$$\phi = \frac{2\pi a R B_\infty}{\pi a R^2 S_{\text{in}}} = \text{ratio of the mass of sulfur on the surface of the pores}$$

to that in the pore volume.

With these definitions, we have

$$\alpha = \theta \left(\frac{t_{\text{bed}}}{t_{\text{diff}}} \right), \quad \beta = \phi \left(\frac{t_{\text{diff}}}{t_{\text{rxn}}} \right).$$

This is one interpretation of the parameters, but others could be considered by grouping the parameters differently. Estimates for these parameters will be given later.

1.2 Numerical approach

The model equations in (7) and (8), along with initial and boundary conditions in (10), are readily solved using a straightforward numerical approach based on finite differences. Consider a Cartesian mesh in the x and z directions with mesh spacings $\Delta x = 1/N$ and $\Delta z = 1/M$, respectively, for chosen positive integers N and M . On the mesh, define

$$\tilde{S}_j(t) \approx S(x_j, t), \quad \tilde{C}_{j,k}(t) \approx C(x_j, z_k, t), \quad \tilde{B}_{j,k}(t) \approx B(x_j, z_k, t),$$

where $x_j = j\Delta x$ and $z_k = (k - 1/2)\Delta z$, and we let t remains continuous for now. It is convenient to define the grid lines in z so that they straddle the boundaries at $z = 0$ and $z = 1$. At a time t , approximate the equations in the bed and the pore using standard second-order finite differences, namely,

$$\frac{\tilde{S}_j - \tilde{S}_{j-1}}{\Delta x} = \frac{\alpha}{2} \left(\frac{\tilde{C}_{j,1} - \tilde{C}_{j,0}}{\Delta z} + \frac{\tilde{C}_{j-1,1} - \tilde{C}_{j-1,0}}{\Delta z} \right), \quad j = 1, 2, \dots, N, \quad (11)$$

with inlet condition $\tilde{S}_0 = 1$, and

$$\frac{\tilde{C}_{j,k+1} - 2\tilde{C}_{j,k} + \tilde{C}_{j,k-1}}{\Delta z^2} = \beta\tilde{C}_{j,k}(1 - \tilde{B}_{j,k}), \quad j = 0, 1, \dots, N, \quad k = 0, 1, \dots, M, \quad (12)$$

with boundary conditions

$$\frac{\tilde{C}_{j,1} + \tilde{C}_{j,0}}{2} = \tilde{S}_j, \quad \frac{\tilde{C}_{j,M} - \tilde{C}_{j,M-1}}{\Delta z} = 0, \quad j = 0, 1, \dots, N.$$

Assuming $\tilde{B}_{j,k}(t)$ is known on the grid at time t , the discrete equations in (11) and (12), along with the inlet condition and boundary conditions, can be solved to obtain $\tilde{S}_j(t)$ and $\tilde{C}_{j,k}(t)$. (These grid functions are easily found by marching in j from $j = 0$ to $j = N$, and solving the linear tridiagonal system implied by (12) and its boundary conditions at each step.) Given $\tilde{C}_{j,k}(t)$, the equation to advance the surface concentration in time is

$$\frac{d}{dt}\tilde{B}_{j,k} = \tilde{C}_{j,k}(1 - \tilde{B}_{j,k}).$$

This equation may be integrated from a given time t to a new time $t + \Delta t$ in a many ways. For example, an explicit second-order accurate Runge-Kutta method involves a two-stage integration. The first stage is

$$\tilde{B}_{j,k}(t + \Delta t/2) = \tilde{B}_{j,k}(t) + \frac{\Delta t}{2}\tilde{C}_{j,k}(t)(1 - \tilde{B}_{j,k}(t)), \quad j = 0, 1, \dots, N, \quad k = 0, 1, \dots, M,$$

which gives $\tilde{B}_{j,k}(t + \Delta t/2)$ on the grid, and then $\tilde{S}_j(t + \Delta t/2)$ and $\tilde{C}_{j,k}(t + \Delta t/2)$ can be obtained from (11) and (12) as before. The second stage is

$$\tilde{B}_{j,k}(t + \Delta t) = \tilde{B}_{j,k}(t) + \Delta t\tilde{C}_{j,k}(t + \Delta t/2)(1 - \tilde{B}_{j,k}(t + \Delta t/2)), \quad j = 0, 1, \dots, N, \quad k = 0, 1, \dots, M,$$

which results in $\tilde{B}_{j,k}$ at the new time level $t + \Delta t$. The process can now be repeated to a time $t = t_{\text{final}}$ given by

$$\tilde{S}_N(t_{\text{final}}) = S_{\text{tiny}},$$

where S_{tiny} is a dimensionless threshold concentration indicating that an unacceptable level of sulfur has broken-out from the end of the packed bed. We use $S_{\text{tiny}} = 0.001$ in the simulations presented in the next section.

1.3 Numerical simulations

We begin with simulations of the behavior of the packed bed in the field. For these simulations, we take

$$\alpha = 5, \quad \beta = 200.$$

These values were obtained by discussions with the representative from Bloom, and by fits to observations of their packed beds in the field. The calculations use $N = 1000$ and $M = 50$ for the number of mesh cells in the x and z directions, respectively, and a time step $\Delta t = 0.02$. The break-out time, t_{final} , for the simulation was found to be 524.3 days in dimensional units.

Figure 1 shows the behavior of $S(x, t)$ at five times with the final time equalling t_{final} . The graph on the left is the solution from the present simulation using the values of α and β fit to the packed beds in the field, while the graph on the right is the solution from the simulation using parameters based on the lab conditions (to be discussed below). We note an apparent traveling wave in $S(x, t)$ with a near linear profile within the active layer of pellets as this layer moves down the packed bed for both simulations.

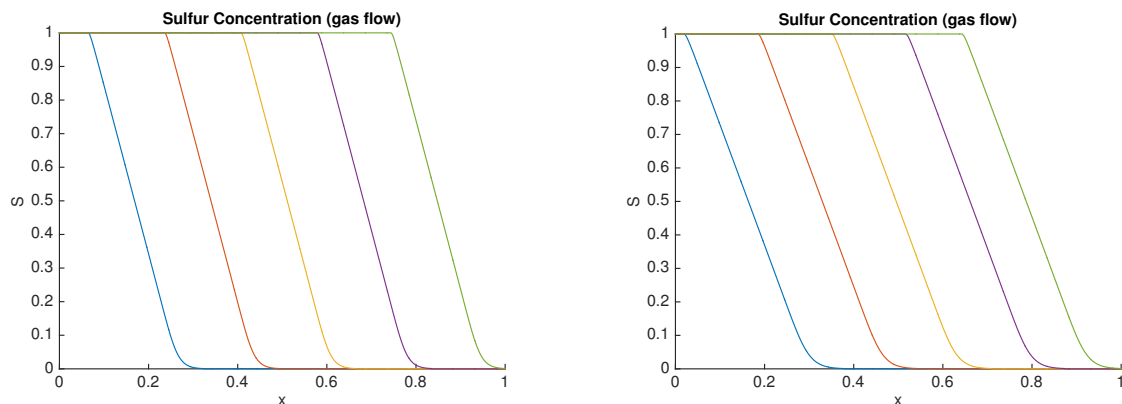


Figure 1: Behavior of $S(x, t)$ for five intervals of time from $t = 0$ to $t = t_{\text{final}}$. Left: field simulation, $t_{\text{final}} = 524.3$ days. Right: lab simulation, $t_{\text{final}} = 0.6854$ days.

Figure 2 shows the sulfur concentrations in pore given by $C(x, z, t)$ and on the pore surface given by $B(x, z, t)$ at two values of time. Upstream of the active layer of the packed bed, both the pore and surface concentrations of the sulfur are saturated at a value equal to one (approximately), while far downstream of the active layer their values are zero. Within the active layer, the concentration of sulfur in the pore decreases with z for a fixed x and t due to the transfer of sulfur to the surface of the pore. The surface concentration also decreases with z for a fixed x and t as the reaction is generally strongest near the inlet to the pore where there is more sulfur available.

To perform experiments in the lab that model conditions in the field, it is important to keep the dimensionless parameters α and β the same, or at least approximately the same, in the model. According to the definitions of these two parameters in (9), we first note that β depends on quantities that pertain to the pellets alone. Thus, if the pellets used in the field

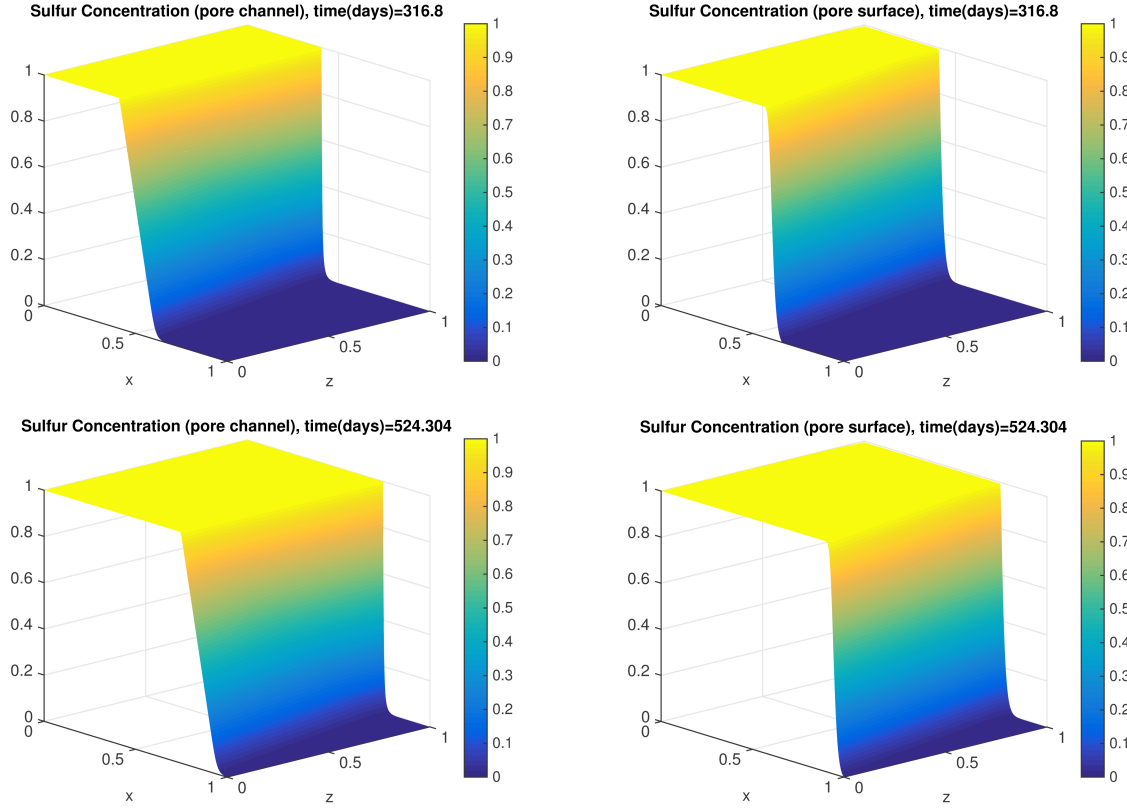


Figure 2: Field simulation: Behavior of the concentration of sulfur in the pore $C(x, z, t)$ (left) and on the pore surface $B(x, z, t)$ (right) at $t = 316.8$ days (top) and $t = t_{\text{final}} = 524.3$ days (bottom).

are the same as those used in the lab experiments, then the value of β would remain the same. The definition of α , on the other hand, involves quantities that depend on the pellets and quantities that involve the geometry and flow in the packed bed. In particular, we can re-write α as

$$\alpha = \left(\frac{AL}{Q} \right) \left(\frac{N\sigma D}{a} \right),$$

where the quantities in the first parentheses depend on the conditions of the bed, while the quantities in the second depend on the pellets alone and would remain unchanged. In the lab experiments, the length of the bed given by L is shorter, 0.15 m in the lab versus 1.7 m in the field, and the velocity of the flow given by Q/A is decreased, 0.05 m/s in the lab versus 0.4 m/s in the field, according to the values supplied by Bloom. Thus, AL/Q is approximately unchanged so that the value $\alpha = 3.59$ used for the simulation of the conditions in the lab is nearly equal to $\alpha = 5$ used for the simulations of the field conditions. Also, it is desirable to obtain results of the lab experiments over a much shorter time than the break-out time (approximately a year) in the field. This can be done by increasing the inlet

concentration of sulfur so that the time scale given by t_{rxn} in (6) is decreased.

The graph on the right in Figure 1 shows the behavior of $S(x, t)$ for $\alpha = 3.59$ and $\beta = 200$ at five times with the final time being $t_{\text{final}} = 0.658$ days. We observe that the qualitative behavior of the sulfur concentration is similar for both the field and lab simulations, as expected. Since the value for α is slightly smaller for the lab simulation, the width of the active layer is larger. This observation is consistent with the equation in (7) describing the balance between the flux of sulfur down the packed bed and the flux of sulfur into the pores of the pellets. If α is smaller, then the flux into the pores is smaller, and thus the width of the active layer becomes larger.

1.4 Concluding remarks

A relatively simple mathematical model has been considered that describes the desulfurization of a one-dimensional gas flow through a packed bed. The model involves several parameters, but these group into two dimensionless parameters upon rendering the model dimensionless. The two parameters depend on the length, cross-sectional area, and the volume flow rate in the packed bed, and on the materials used to pack the bed (pellets). Once these parameters are found for the conditions of the packed bed in field, they provide a guide to scale the experimental set-up to study the behavior in the lab.

A straightforward numerical approach has been implemented in MATLAB to obtain solutions of the model. These simulations determine the time-dependent concentration of sulfur in the bed, and the sulfur concentration in the pores of the pellets. By computing the sulfur concentration at the end of the bed, the break-out time when the concentration rises above a specified threshold can be determined. Results of the simulations are in good qualitative agreement with the observed behavior of the packed beds in the field.

Extensions of the model can be made. For example, a straightforward extension of the model and numerical scheme would allow for the simulation of packed beds containing regions with pellets of different properties. The two parameters, α and β would become functions of x , the distance down the bed, in this case. The current model assumes a one-dimensional flow of gas down the bed. This assumption could be lifted, but this would make the model, and corresponding numerical approach, more difficult. It was generally agreed that this extension would need to be made in order to obtain higher fidelity in the predictive capabilities of the model.